Spin-Orbit and Spin-Spin coupling in the triplet state

Sathya Sai Ramakrishna Raj Perumal

Doctoral Thesis in Theoretical Chemistry and Biology

Stockholm Sweden 2012

PhD disertation
Department of Theoretical Chemistry and Biology
School of Biotechnology
KTH Royal Institute of Technology
114 21 Stockholm Sweden
Coverpage: Spin-density contour of nanographene ribbon with defect, Breit-Pauli Hamiltonian for Spin-Orbit coupling and electronic spin-spin dependence on the size of nanotubes

ISBN 978-91-7501-366-4
Printed by Universitetservice US AB
Stockholm 2012

எப்பொருள் யார்யார்வாய்க் கேட்பினும் அப்பொருள்
மெய்ப்பொருள் காண்ப தறிவு.

திருக்குறள் - 423

The mark of wisdom is to discern the truth
From whatever source it is heard.

Thirukural - 423

ABSTRACT
SPIN-ORBIT AND SPIN-SPIN COUPLING IN THE TRIPLET STATE
Sathya S. R. R. Perumal
Department of Theoretical Chemistry and Biology
KTH Royal Institute of Technology Stockholm Sweden

The underlying theory of "Spin" of an electron and its associated interactions causing internal fields and spectral shift to bulk-magnetism is well established now. Our understanding of spin properties is significant and more useful than ever before. In recent years there seems to be an enormous interest towards application oriented materials that harness those spin properties. Theoretical simulations remain in a position to "assist or pilot" the experimental discovery of new materials.

In this work, we have outlined available methodologies for spin coupling in multi-reference and DFT techniques. We have benchmarked multi-reference spin-Hamiltonian computation in isoelectronic diradicals - Trimethylenemethane (TMM) and Oxyallyl. Also with DFT, parameters are predicted with a newly discovered TMM-like stable diradicals, reported to have large positive exchange interactions. Excellent agreement were obtained and our findings emphasize that the dipole-dipole interactions alone can predict the splitting of triplet states and that DFT spin procedures hold well in organic species.

We have extended our spin-studies to a highly application oriented material - nanographene. Using our novel spin-parameter arguments we have explained the magnetism of graphene. Our studies highlight a few significant aspects - first there seems to be a size dependency with respect to the spin-Hamiltonian; second, there is a negligible contribution of spin-orbit coupling in these systems; third, we give a theoretical account of spin restricted and unrestricted schemes for the DFT method and their consequences for the spin and spatial symmetry of the molecules; and, finally, we highlight the importance of impurities and defects for magnetism in graphene. We predict triplet-singlet transitions through linear response TDDFT for the tris(8-hydroxyquinoline) aluminium complex, an organic molecule shown to have spintronics applications in recent experiments. Our spin studies were in line with those observations and could help to understand the role of the spin-coupling phenomena.
Keywords Spin-Spin, Spin-Orbit, D and E parameters, ZFS, graphene, TMM, OXA, diradicals, tris(8-hydroxyquinoline) aluminium, magnetic anisotropy, magnetism, triplet

PUBLICATION LIST

I Spin-spin coupling in $^3b_2$ state of oxyallyl - A comparative study with trimethylenemethane
S. Perumal, B. Minaev, O. Vahtras and H. Ågren
Computational and Theoretical Chemistry, 963 (51-54) 2011
Included for Lic. Work

II Zero-Field Splitting of compact trimethylenemethane analogue radicals with density functional theory
S. Perumal
Chemical Physics Letters, 501 (608-611) 2011

III Spin-spin and spin-orbit interactions in nanographene fragments: A quantum chemistry approach
S. Perumal, B. Minaev, H. Ågren
Journal of Chemical Physics,* 136,*104702, 2012

IV Modeling the triplet states of the tris(8-hydroxyquinoline) aluminium (Alq_3) complex
S. Perumal, B. Minaev, H. Ågren
manuscript

CONTRIBUTION

I declare for all the projects design, work-flow of the calculations, interpretation of the theoretical results, literature survey of the earlier methods and write up for a publishable manuscript was accomplished by me. For Paper I, I have contributed significantly for the write-up along with co-authors. For Paper II from design to publishable manuscript was accomplished by me. For Paper III the project was conceived, designed by me and publishable manuscript was accomplished by me with contributions from other co-authors. For paper IV the project was conceived, designed by me for calculations with contributions from other co-authors for the manuscript.

Notations and Abbreviation

1. SSC - Spin-Spin coupling(electron-electron)
2. SOC - Spin-Orbit coupling
3. ZFS - Zero-field splitting
4. TMM - Trimethylenemethane
5. OXA - Oxyallyl
6. Alq_3 - Tris-hydroxy Aluminium 8-oxalate
7. MCSCF - Multiconfigurational Self-Consistent Field
8. η - SOC constant
9. α - fine structure constant
10. SMM - Single Molecule Magnet
11. ρ_e - electron density
12. $\boldsymbol{J}$ - Exchange interactions
13. $\sigma_{x,y,z}$ - Pauli Matrices
14. ∇ - Gradient Operator
15. χ - Spinors

Contents

Chapter 1

Introduction

Information is fundamental.[1] In a well-connected post modern civilization the flow of information has truly revolutionized mankind. It has been predicted that the amount of information around the world increases by 40% annually. At a basic level this information is represented by ones and zeros. Just like the speed of processors increases by following the Moore's law, the ability to pack huge chunks of data into a tiny volume has improved over the years. Eventually the physical limit of this tiny volume would be at the atomic or molecular level.

Looking back in history it was a break-through to represent information in magnetized domains. With the limitation of punched cards in the early years, tape drives were used (1950's).[2] Later the technology of magnetoresistance - change of resistance with respect to external magnetic field - was employed in the hard-disk drive. A very high-density packing of data was achieved by the "Giant- magnetoresistance(GMR) technique" - discovered by A. Fert and P. Grünberg.[3, 4].

Over six decades the size of the domains has decreased tremendously from a few millimeters to nanometers (billion fold in scale). From these achievements it is not surprising if at some point in the future we are reaching the atomic or molecular limit to store information represented by ones and zeros.

Researchers believe this could be possible by designing a molecule to act as a miniature sized bar magnet,[5, 6], classically speaking, two possible orientations of tiny magnets (the magnetic moment of the total spin of a molecule) would act as representations of one and zero.

The "Nature" solution for storing the genetic information codes of life were in the form of RNA and DNA

Scaling from the bulk dimensions to the smaller units, "isolated molecules and collection of molecules can exhibit magnetic properties, often referred to the term *Molecular Magnetism*".[7]

"Reducing the bulk properties of Ferromagnetism to magnetic materials of mesoscopic dimensions (10 $\mathring{A}$ to 100 $\mathring{A}$) gives pronounced hysteresis and can be used as bistable magnetic units for data storage", as proposed by Sessoli *et al.*[5] The hunt for such assembly of magnetic molecules started a couple of decades ago and was discovered by Sessoli *et al* in 1993, with very high spin $S = 10$ for the Mn_{12} single molecular complex, however, at very low temperature (4 K). Yet it is a remarkable breakthrough on the way for practical single molecular magnets (SMM). An important characteristic of such a molecular magnet is to possess slow relaxation of the magnetization so that it remains magnetized for long times.[8]

1.1 Exchange Interaction

The Heisenberg spin Hamiltonian to describe interacting spins is

$$H = -\sum_{i,j} 2J_{ij}\mathbf{S_i}\mathbf{S_j} \tag{1.1}$$

In Eq 1.1 the spin interaction is isotropic and represents interaction of the spin vectors S_i and S_j located in the nearest-neighbor sites i and j, respectively. $\boldsymbol{J}$ is the *Heisenberg exchange constant*, where positive $\boldsymbol{J}$ means ferromagnetic interaction of spins and negative $\boldsymbol{J}$ means anti-ferromagnetic interaction of spins. However, very often the spin-interactions are anisotropic due to environmental effects, leading to modification of the above equation as

$$H = -\sum_{i,j} 2J_{i,j}[S_i^z S_j^z + \gamma(S_i^x S_j^x + S_i^y S_j^y)] \tag{1.2}$$

where γ represents a generalization of the interactions. For example Eq 1.1 is a special case of Eq 1.2 if one substitutes $\gamma = 1$. $\gamma = 0$ leads to Ising spin interactions while $\gamma >> 1$ represents two-dimensional spin interactions. The spin Hamiltonian above can be incorporated in terms of isotropic spin-spin interactions (Heisenberg Hamiltonian as in Eq 1.1) and single-ion anisotropy terms.

$$H = -\sum_{i,j} 2J_{i,j}\mathbf{S_i}\cdot\mathbf{S_j} - D\sum_i (\hat{\mathbf{u}}_\mathbf{i}\cdot\mathbf{S_i})^2 - g\mu_B\sum_i \mathbf{H}\cdot\mathbf{S_i} \tag{1.3}$$

where D is the measure of anisotropy strength of the spin orientation S_i with respect to the unit vector $\hat{u}_i$, thus representing the anisotropy term; the first term corresponds to the isotropic Heisenberg Hamiltonian; the last term is the *Zeeman interaction* in the presence of an external field **H** with the constant called *g-factor*.

The anisotropy(second term) describes two interesting spin interactions - spin-orbit and spin-spin coupling. These two terms play a significant role in deciding the magnetic anisotropy parameters. The dominance of either one of the coupling depends on the particular system. For the case of metallic complexes spin-orbit predominantly decides the strength of anisotropy parameters since the presence of unpaired *d-orbital* electrons and hence availability of higher angular-momentum, whereas in organic species the angular momentum contribution comes from the *p-orbital* electrons with negligible contribution from the SOC effect. Often in the case of organic species the SSC dominates as shown in this work.

With the availability of very sensitive magnetic field measurements using *superconducting quantum interference device* (SQUID), measurement of alternating current(AC)/direct current(DC) magnetic susceptibility of SMMs is possible in a cryogenic environment (temperature as low as $1.7K$), often accompanied with single crystal magnetization measurement with micro-SQUID[9]. From experimental susceptibility $\chi_{mol}(T)$ versus temperature plots, theoretical fits are done to obtain the exchange constants. From measurement of magnetization(M) versus magnetic field (H) yields the necessary fits for total ground state of spin, zero-field splitting(ZFS) D tensor, E tensor and *g-factor*. This is accomplished by the use of the following relation that employs standard statistical partition function.[10] However the main bottleneck is that the cost of diagonlization rapidly increases as the eigenspace of spin (S) increases.

$$\chi_{mol} = -\mu_0 N_A \frac{\sum_n [(E_n^1)^2/kT - 2E_n^2] e^{(-E_n^0/kT)}}{\sum_n e^{(-E_n^0/kT)}} \tag{1.4}$$

where energy the eigenvalues E_n where used until second order.

We can isolate the second term in Eq 1.3 for our description and with proper choice of coordinate system it can be diagonalized as

$$H_{zfs} = D[S_z^2 - \frac{1}{3}S(S+1)] + E(S_x^2 - S_y^2) \tag{1.5}$$

In the first term of Eq 1.5 S_x, S_y and S_z are the components of spins, and the parametrized D and E essentially defines the magnetic anisotropy. In other terms, these parameters describe the strength of splitting of the multiplets in the absence of any external magnetic field or zero magnetic

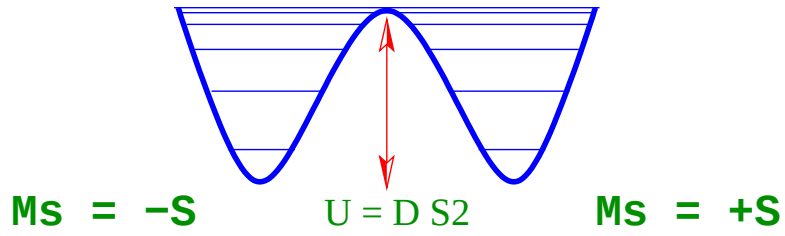

Figure 1.1: Simplified double well approximation with barrier DS^2

Table 1.1: Typical barrier energy for SMM

Complex	D_{expt} (cm^{-1})	S	DS_z^2 (cm^{-1})	Ref.
Mn_{12}(acc.)	-0.46	10	46	[11]
Mn_6	-0.43	12	62	[12]
$Mn(acac)_3$	-4.52	2	18	[13]
Fe_8	-0.30	10	30	[14]

field. In simple terms we can visualize the magnetic anisotropy barrier as the energy to cross the wall between a approximate symmetric quantum mechanical double well potential and can be quantified as DS_z^2. (see fig. 1.1 Thus for a practical SMM the D parameters should be negative i.e. $D < 0$, with the z-axis out of plane. For example, Table 1.1 lists the parameters for typical cases of SMM:s reported in the literature.[11, 12, 13, 14]

Over the years the techniques to probe such magnetic complexes has improved both in experiment and in theory. There has been lots of SMMs reported so far in the literature ranging from transition metals to lanthanides.

Eq 1.5 is tradtionally used to describe the splitting ("fine structure") of the degeneracy of multiplets of the molecules due to internal fields arising from the spin interactions and has been used for the fitting EPR or ODMR spectra of diradicals or paramagnetic species. One can observe ZFS in any molecule with ground state spin $S > 1/2$.A very good review by Boča discuss the issue of ZFS and connection to the magnetism.[15]. However van Wullen has proposed that the connection between the zfs barrier and magnetic-anisotropy should be taken cautious.[16] For example let us consider the case of the oxgyen (O_2) molecule, where the ground state is paramagnetic, defined by the $^3\Sigma_g^-$ state. The two unpaired π^* valence electrons couple each other and cause an effective internal magnetic moment and hence their triplet degeneracy is broken.(shown in the Fig 1.2. The splitting strength is observed to be $D = +3.96cm^{-1}$ in the microwave EPR measurements.[17] The fine structure splitting in the spectra can be accounted for by Eq 1.5 with proper choice of diagonilzation axes. In the case of O_2 the *z-axis* is assumed to be

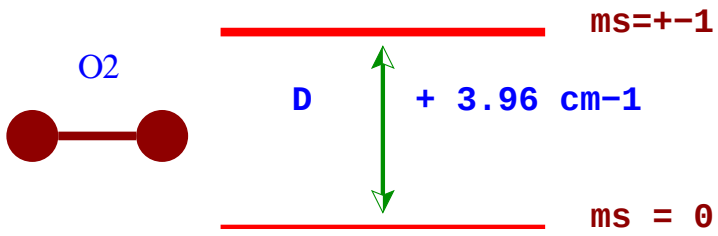

Figure 1.2: Schematics of broken degeneracy of triplet ground state O_2

the principle axis of the molecule, *i.e.* E is zero for the case of O_2.

Typical magnitudes of spin interactions is given by[18]

1. electronic Zeeman interaction - 1 cm^{-1} (10^4 gauss)
2. magnetic hyperfine interaction - 10^{-1} cm^{-1} (10^3 gauss)
3. nuclear Zeeman interaction - 10^{-3} cm^{-3} (10^6 gauss)

1.2 Current status

In quantum chemical problems, very often relativistic effects are neglected in main-stream energy calculations and successive property predictions, often justified with the notion of small additional effects on the unrelativistic Hamiltonian. With the pioneering works of Pyykkö the significance of relativistic effect has been emphasized in particular for first-principle quantum chemistry.[19, 20]

> Pyykkö could show that without relativistic effects
> lead batteries used in cars would behave just
> like tin and never ignite "and so cars start due to relativity" [21]

The neglect of relativistic effects are indeed important for the cases like inter-system crossings a phenomenon of crossing of potential energy surface between two different multiplets; ISC occurs in chlorophyll, human eye, and is strong in valence shells of heavy elements and causes fine structure splitting in light elements, phosphorescence, SMM, etc. The theory is capable of including relativistic effect in calculations involving post-Hartree-Fock methods like MCSCF, CASPT, CCSD with a wide range of techniques from perturbation to four-component approach, though it takes extra effort computationally.

An extensive review of inclusion of relativistic effects in quantum chemistry can found in Ref. [22, 23, 24, 25, 26, 27] First principle calculations for the case of the H_{zfs} spin Hamiltonian have received significant attention in the past two decades, especially in the context of SMM applications. H_{ZFS} has two significant contributions; from SSC (first-order contribution) and SOC (second-order contribution). Post-Hartree-Fock methods include an excellent way of predicting the spin-coupling properties (here we refer to SSC and SOC), by incorporating the relativistic equation in the Self-Consistent Field (SCF) procedures.

Modern quantum chemistry and condensed-matter physics have benefited enormously from the advent of density functional theory based approaches. Massive scaling for prediction of properties for systems of interest is now readily available with sophisticated techniques like linear scaling, plane-wave pseudo potential and Car-Parinello Molecular Dynamics calculations, though all the properties of interest are not included. Accurate descriptions of spin properties, which essentially gives the magnetism, still remains a challenge. An efficient and accurate description of Eq 1.5 still remains an elusive procedure in DFT. Nonetheless there has been tremendous progress in these aspects.

The first description of modelling the anisotropy parameter was put forward by Pederson *et al.*.[28, 29] Anisotropy parameters of Mn_{12}(acct) SMM complexes were modelled successfully by treating the SOC effect as a perturbation in the regular Kohn-Sham procedures, thus treating $\hat{L} \cdot \hat{S}$ as perturbation to the DFT wave function. Although their approach was good in modelling a few high-spin complexes, it has a short-coming with improper account of prefactors, which was later rectified by Neese. And Neese himself proposed another technique - QRO in DFT for calculating the parameters for SMM. A brief account of both methods is given in Chapter 2.

Molecular magnetic materials are also thought to play an important role in molecular spintronics - acting as a bridge between spintronics and molecular electronics as proposed by Bogani *et al.*[30]. In their article Bogani *et al* review the challenges faced in realizing such practical electronic devices. They suggest that extremely low-temperature operational SMMs may not be practical in everyday electronics. However, they can help understanding fundamental physics and consequences of their applications.[30]

Enhanced magnetic anisotropy has also been reported in surface interfaces as well. Gambardella *et al.* have reported giant magnetic anisotropy of single cobalt atoms when deposited on the surface of Platinum(Pt) (111) surface.[31] The MAE of bulk Co is 0.045 meV and when placed in array on the Platinum surface, an enormous enhancement of MAE, 9 meV, has been reported. The giant increase in MAE is essentially attributed to the spin-

orbit coupling and stems from 5d-orbitals of Pt. This has been extended for dimer and trimer of Cobalt and Iron atoms and the stability of such species for atomic level MAE has been analyzed.[32] Atomic cluster based MAE calculations have been done with a *Chern number* spin Hamiltonians approach by Canali and co-workers, their approach also reports the physical limit of MAE for transition-metal dimers.[33] Similarly, theoretical predictions elsewhere reports on 3d, 4d,5d metal dimers with DFT based methods predicting potential atomic scale molecular magnets.[34, 35, 36, 37] A number of hybrid system involving a sandwich of metal and organic species with pronounced theoretical prediction of MAE also looks promising in this fascinating field of SMM.[38, 39, 40, 41]

In addition to the transition metal series there has been a number of reports on *f-block* lanthanides based SMMs. Single Erbium ion based compact organometallic magnets with remarkable magnetic characteristics has been synthesized by Gao workers in 2011.[42] The unusual features of this SMM is that it shows magnetism in the higher temperature range("with two thermal magnetic relaxation process as high as 197 and 323 K").[42] A very detailed review of lanthanide based SMMs has been reported by Sessoli *et al.*[43]

In an interesting report Liddle *et al.* have reported Uranium based SMMs[44], where the conventional theoretical explanation of super-exchange interactions fails for this diuranium complex through the dianionic arene and it remains an open question to explain the spin-coupling of this *f-block* SMM.

Tuning the anisotropy parameters by electric field also seems to be another aspect proposed for controlling the SMM for desired characteristics.[45] The problem of occurence of high-spin and anisotropy has been dealt with in detail in Ref. [46]

The presence of only p and s electrons in the organic material limits the scope of ferromagnetism. However there has been lots of attention in synthesizing organic radicals which have unpaired electrons that can be exploited for the desired magnetic features. Though most of the SMMs are based on inorganicis very often their interactions occurs through organic groups.[47] Reviews of organic magnetism can found in Ref. [48] and organic diradical based magnetism in Ref. [49]

Indeed, this field evolving owing to the richness of a wide variety of underlying physics - many different quantum phenomena are associated with SMM:s. Though in short time there has been scores of syntheses of SMM:s probing the quantum processes, the number of theoretical studies does not match the experimental counterpart by far. This is mainly due to unavailability of accurate schemes to describe the high-spin multi-nuclear complexes and the corresponding description of multi-body correlation. Yet this emphasizes the need for sufficient theoretical tools to understand and disseminate

the molecular level behavior of magnetism with mathematical rigour.

This thesis work is a very humble effort in explaining specific questions concerning spin behavior in the systems of interest.

Chapter 2

Theoretical Methods

Theoretical modelling with account of relativistic effects is carried out using many types of approximations in quantum chemistry, often accounted for in the regular non-relativistic approximations by means of perturbation theory. The accuracy of such calculations depends on the how accurate the quantum states are in the non-relativistic regime. Multireference correlation methods are a good choice if one desires an accurate description of ground or low-lying excited states. We need sophisticated techniques to deal the spin-Hamiltonian calculations in DFT as in the case of post-Hartree-Fock methods. In this chapter we briefly go through available techniques for the spin-Hamiltonian implementation both in post-Hartree-Fock and DFT schemes. Our objective here is to utilize the total Hamiltonian for any quantum chemical system including the relativistic terms.

$$\hat{H} = \hat{H}_0 + \hat{H}_{so} + \hat{H}_{ss} + \hat{H}_{hyperfine} + \hat{H}_{Darwin} + \hat{H}_{mass-velocity} \tag{2.1}$$

where $\hat{H}_0$ is the non-relativistic Hamiltonian, $\hat{H}_{so}$, $\hat{H}_{ss}$ are spin-orbit and spin-spin terms, and remaining terms are hyperfine - arising from interaction with the nuclear moment, Darwin and mass-velocity terms, respectively. As we discussed earlier in the introduction the emphasis of this thesis is on the spin-orbit and spin-spin Hamiltonian. We discuss in this chapter the underlying theory for evaluating corresponding terms in first-principle calculations.

2.1 Breit-Pauli Hamiltonian

The full spin-orbit Hamiltonian is given by

$$\hat{H}_{so} = \frac{\alpha^2}{2} \sum_{iN} \frac{Z_N}{r_{iN}^3} (\hat{r}_{iN} \times \hat{p}_i) \cdot \hat{s}_i - \frac{\alpha^2}{2} \sum_{i \neq j} \frac{1}{r_{ij}^3} (\hat{r}_{ij} \times \hat{p}_i) \cdot (\hat{s}_i + 2\hat{s}_j) \tag{2.2}$$

Eq 2.2 can be divided into one-electron, spin-own and spin-other-orbit interactions. spin-orbit interactions. In quantum chemistry this Hamiltonian is most often regarded as a perturbation of unperturbed wavefunctions (Ψ_0). The spin-orbit operator in its simplest form is often written

$$\eta \hat{L} \cdot \hat{S} \tag{2.3}$$

In order to evaluate this Hamiltonian in quantum chemical calculations of molecular properties (spectral splittings etc.) one has to do a proper implementation that balances speed and accuracy.

The inclusion of the spin-orbit Hamiltonian above is not necessary for regular energetics, often the energy correction introduced is negligible, (typically of the order of $\sim eV$), thus the major part of quantum chemistry literature seldom includes relativistic corrections. However for spin properties like spectral splittings the spin-orbit Hamiltonian accounts for a significant role in explaining the spectroscopy. In conventional post Hartree-Fock procedures its implementation is well established.

Before describing a few successful methods tackling Eq 2.2, let us draw our attention to the practical difficulty on algorithmic implementations. Eq 2.2 Computing the one-electron part of the Eq 2.2 is straightforward. The computation of the two-electron term involves substantial computational time and is generally a small contribution to the total Hamiltonian, while a major contribution arises from the one-electron term alone. Here we discuss two different established methods

2.2 Spin-Spin Coupling

> The notion of "magnetic dipole interaction depends only on the components of two-particle density matrix that are antisymmetric in the space variables" was proposed and proved to be a theorem by McConnell in a classical work.[50]

Along with the Breit-Pauli Hamiltonian there is another contribution, the spin-spin Hamiltonian. Although being generally a negligible contribution, particularly in organic molecules it plays a vital role in degeneracy splittings.

$$\hat{H}_{ss} = \frac{\alpha^2}{2} \sum_{i,j} \left[\frac{\vec{s}_i \cdot \vec{s}_j}{r_{ij}^3} - \frac{3\left(\vec{s}_i \cdot \vec{r}_{ij}\right)\left(\vec{s}_j \cdot \vec{r}_{ij}\right)}{r_{ij}^5} \right] \tag{2.4}$$

Eq 2.4 very much resembles the classical analogue - dipole-dipole interactions. The calculation of Eq 2.4 is straightforward and can be diagonalized in parametrized form.

The ZFS tensor D_{ij} is in our implementation given by

$$D_{ij} = \sum_{\mu\nu\rho\sigma} d_{ij,\mu\nu\rho\sigma} q_{\mu\nu\rho\sigma} \tag{2.5}$$

where $q_{\mu\nu\rho\sigma}$ is a two-electron density matrix and $d_{ij,\mu\nu\rho\sigma}$ is the integral of i and j'th Cartesian component of the two-electron field gradient operator over μ, ν, ρ, σ indexed orbitals. Eq 2.5 reduces for non-zero values of the quintet density to

$$D_{ij} = \frac{1}{2} \sum_{\mu\nu\rho\sigma} d_{ij,\mu\nu\rho\sigma} (P_{\mu\nu} P_{\rho\sigma} - P_{\mu\sigma} P_{\rho\nu}) \tag{2.6}$$

where P is the *active* density matrix in atomic orbitals given in terms of molecular orbital co-efficients C_{ij}

$$P_{ij} = \sum_{k} C_{ik} C_{kj} \tag{2.7}$$

The biradicals has a triplet ground state, and this reference state can be generated through multi-reference calculations or through density functional theory.

$$H_{ij} = \langle {}^3\Psi_0 | H_{ss} | {}^3\Psi_0 \rangle \tag{2.8}$$

In parameter form anisotropy tensors are given by

$$D = \frac{3}{2} D_{zz} \tag{2.9}$$

$$E = \pm \frac{1}{2} (D_{xx} - D_{yy}) \tag{2.10}$$

This method of implementation for dipole-dipole computations is available in DALTON.[51] This method of implementation for dipole-dipole computations is available in DALTON.[51]

2.3 Mean-Field Approximation

Hess *et. al* constructed an effective one-electron spin-orbit Hamiltonian by averaging the two-electron contributions to the spin-orbit matrix element over the valence shell.[52] In doing this they only considered the one-center

terms. In their work, Eq 2.2 assumes the following form when it connects the Slater determinant that differs by a single valence orbital excitation.

$$H_{ij}^{mean-field} = \langle i|H^{so}(1)|j\rangle + \frac{1}{2}\sum_{k} fixed(n_k)(\langle ik|H^{so}(1,2)|jk\rangle \quad (2.11)$$

$$-\langle ik|H^{so}(1,2)|kj\rangle - \langle ki|H^{so}(1,2)|jk\rangle) \quad (2.12)$$

where the excitation is from i to j. for example singlet to triplet, triplet to pentet and so on. n_k is the common number occupancy of both determinants. Thus Eq. 2.11 elegantly put the motion of a valence electron in the average field of occupied orbitals forming an independent-particle approximation.

Hess *et. al* point out that the choice of specific occupation number needs to be checked since the occupation also includes the valence shell and a small dependence of valence orbital occupation is anticipated. The multi-centre two-electron integrals are discarded defining an effective one-electron operator. In their original work very good agreement was obtained with the mean-field one-centre approximation comparing with the full-breit Hamiltonian for the benchmark case of a relativistic element such as Pladium(Pd). In the following table we report calculated spin-orbit matrix elements with full and mean-field one-centre approximation for selected species in order to illustrate the effect of the approximation.

Molecule/Matrix element	Type	SOC (cm^{-1})	Ref.
PtH			[53]
$\langle^2\Delta_{5/2}\|H_{so}\|^2\Delta_{5/2}\rangle$	full-breit	-4047	
	mean-field	-4046	
	ECP	-4117	
$\langle^2\Delta_{3/2}\|H_{so}\|^2\Pi_{3/2}\rangle$	full-breit	-4054	
	mean-field	-4054	
	ECP	-4126	
O_2			[54]
$\langle^1\Sigma_g^+\|H_{so}\|^3\Sigma_g^-\rangle$	one-electron(Response)	251.25	
	two-electron(Response)	-94.43	

Table 2.1: Mean-field Spin-Orbit approximation for few species

The mean-field approximation seems most popular for many *ab initio* implementations involving the SOC effect. This is evident from the number of citations to the original work of Hess *et. al* has received over the years (cited 298 times, from web of science-2011[55]). It is worth to note that this idea was used for effective calculations of properties such as *Phosphorescence* in the

formalism of linear response theory in DALTON. Apart from DALTON, the mean-field approximation is also available in ORCA, ADF and several other quantum chemistry programs. In this work we have used the concept of a spin-orbit mean-field (SOMF) for approximating the two-electron spin-orbit integrals in a DFT framework.

2.4 Effective Core Potential

Another way of simplifying the two-electron SOC integrals is to use an effective one-electron operator introduced by Koseki *et al.* [56] with an effective nuclear charge (Z_{eff}). The one-electron approximation used in this method is given by

Table 2.2: SOC effect through ECP on the relative placement of energies level

Molecule/Atom	Term Symbol	Relative energy (cm^{-1})	Expt	Ref.
PtH_2	$^3\Delta_g$	5777		[57]
	$^1\Sigma_g$	5833		
	$^3\Pi_g$	8809		
	$^3\Phi_g$	12486		
	$^2\Sigma_g$	13596		
Pt	$^3D_3$	0.0	0.0	[58]
	$^3D_2$	782	775	
	$^3D_1$	10010	10132.00	

$$\hat{H_{so}} = \frac{\alpha^2}{2} \sum_i \sum_A \frac{Z_{eff}(A)}{r_{ij}^3} \hat{L}_{iA} \hat{S}_i \tag{2.13}$$

where Z_{eff} is the *effective nuclear charge* that accounts for an approximate two-electron spin-orbit(other-orbit) interaction. α is the fine-structure constant, L_{iA} is the angular momentum of the electron with respect to the nucleus of the atom. In a series of work Koseki *et al.* have reported Z_{eff} for the elements across the periodic table. [59, 56, 60, 58] ECP method is incorporated in the GAMESS-US program.

A detailed review of MNF and ECP has been reported by Fedorov *et al.* in Ref. [25] and by Marian in an old review in Ref. [26] and in a recent review by the same author in Ref. [61]

2.5 Four-component Dirac Equation

The relativistic analogue of non-relativistic Schrödinger equation was first proposed by Dirac[62] (in 1928) and is given by

$$[c\alpha \cdot \hat{\mathbf{p}} + \beta mc^2]\psi\ (r,t) = ih\frac{\delta\psi(r,t)}{\delta t} \tag{2.14}$$

where ψ is the **four-component** wave function or *field* and α and β 4×4 hermitian matrices possessing specific algebraic identities

$$\alpha = \begin{pmatrix} \mathbf{0} & \sigma_{\mathbf{i}} \\ \sigma_{\mathbf{i}} & \mathbf{0} \end{pmatrix};\ \beta = \begin{pmatrix} \mathbf{i} & \mathbf{0} \\ \mathbf{0} & -\mathbf{i} \end{pmatrix} \tag{2.15}$$

where σ_i are 2×2 Pauli matrices and i runs through (x, y, z) indices.

$$\sigma_x = \begin{pmatrix} 0 & 1 \\ 1 & 0 \end{pmatrix};\ \sigma_y = \begin{pmatrix} 0 & -i \\ i & 0 \end{pmatrix};\ \sigma_z = \begin{pmatrix} 1 & 0 \\ 0 & -1 \end{pmatrix} \tag{2.16}$$

The four-component wavefunction is

$$\psi = \begin{pmatrix} \psi^l \\ \psi^s \end{pmatrix} \tag{2.17}$$

where ψ^l and ψ^s are large and small component of the wavefunction, respectively. Eq. 2.17 accounts for the many-body problem involving particles obeying *Fermi-Dirac statistics*(Fermions - fundamental particles having the half-integer spin(1/2). Inherently the four-component dimensions have the difficulty of being computationally expensive. Further, "Kinetic energy balance procedures" are used to evaluate the Dirac operator.[63, 64] The MOLFDIR code from University of Groningen mainly developed for this approach can solve the four-component Dirac equation.[65] The DIRAC program, mainly a Scandinavian collaboration, has an implementation of the four-component approach.[66]. The Liu group has implemented the linear response time-dependent four-component relativistic DFT method in their BDFT (Beijing DFT) program.[67] In a series of articles, the Liu group has proposed "spin-flip" excitations in the regime of TDDFT.[68, 69, 70, 71]

Gaussian-type four-component spinors allows for calculations of small scale species. An efficient algorithm was proposed by Yanai*et al* for four-component DFT and good performance were achieved in the case of $(SS|SS)$ integrals.[72]

Four-component calculations using the Dirac-Hartree-Fock(DHF)[73] and Dirac-Kohn-Sham(DKS) methods [72], which were developed by Hirao's group

at the University of Tokyo is available in their UTChem program.[74] Spectroscopic properties of certain species have been benchmarked. A detailed review of different implementations of four-component DFT methods can be found in the review reported by Belpassi *et al.*[75]

2.6 Two-component method

A reduction of four-component methods (only for electronic spectrum i.e) ψ^L assuming the systems has no positronic spectra and neglecting quantum electrodynamics effects) into two-component form is another feasible option. A detailed investigation of such two-component spinor transformations is done by Kutzelnigg.[76] The most popular two-component spinor approaches are

1. Zero-order relativistic Hamiltonian.(ZORA)
2. Douglas-Kroll-Hess Approach.(DKH)

2.6.1 Zero-order relativistic Hamiltonian ZORA

The two-component scalar relativistic equation in the ZORA formalism is given by

$$\begin{aligned} H^{\hat{ZORA}} &= \hat{\sigma}\cdot\hat{\mathbf{p}}\frac{c^2}{2mc^2-V}\hat{\sigma}\cdot\hat{\mathbf{p}}+V \\ &= \mathbf{p}\frac{c^2}{2mc^2-V}\mathbf{p}+\frac{c^2}{(2mc^2-V)^2}\sigma\cdot(\nabla\ \mathbf{V}\times\mathbf{p})+V \end{aligned}$$

Eq. 2.18 can be expanded further and be realized to have spin-orbit $\frac{1}{(4m^2c^2)}\sigma\cdot(\nabla\ \mathbf{V}\times\mathbf{p})$, dipole component $\frac{-e\hbar}{2mc}\sigma\cdot\nabla\times\mathbf{A}$ Darwin $\frac{\hbar^2}{8m^2c^2}\nabla^2V$ and Newtonian terms $\frac{p^2}{2m}$ The Amsterdam Density Functional program (ADF) [77], GAMESS-UK [78], GAMESS-US [79, 80]have implementations of the ZORA Hamiltonian in DFT based calculations.

2.6.2 Douglas-Kroll-Hess Approach

This is an approach initially developed by Douglass and Kroll, simplifying the four-component Dirac equation into two-component form. With

unitary transformations (block-diagonalization procedures $U\hat{H}^D U\dagger$) Douglas and Kroll split the total unitary transformation into of series of unitary transformations

$$U = U_n ... U_1 U_0 \tag{2.18}$$

thus the unitary transformation corresponding to the operation U_0 yield first-order Douglas-Kroll Hamiltonian (DK1) ans so forth. U_0 is given by

$$\psi = \begin{pmatrix} A & AR \\ -AR & A \end{pmatrix} \tag{2.19}$$

where

$$A = (\frac{E_0 + c^2}{2E_0})^{1/2} \tag{2.20}$$

$$R = \frac{c\hat{\sigma} \cdot \hat{p}}{E_0 + c^2} \tag{2.21}$$

are kinematical terms

$$E_0 = (p^2 c^2 + c^4)^{1/4} \tag{2.22}$$

The successive mathematical operations using above relations (detailed derivation is out of scope of this summary and we refer for more detail to Ref [81] and Ref [82]) yields the DKH hamiltonian to multiple orders.(H_{DK1}, H_{DK2},etc)

Very recently Nakajima *et al* and Reiher independently have reviewed the DKH approach in detail with connections to practical aspects in Ref. [81] and Ref. [82] respectively. DKH procedures are available in e.g. MOLCAS and GAMESS-US.

2.7 Spin Hamiltonian in the Response Formalism

Physical properties of a system can be thought of as response to external perturbations. Their behaviour with respect to applied fields can be well explained through so called *Response theory*. A general theory for obtaining response properties like linear, quadratic and cubic functions with respect to MCSCF references is well known. [83] The response function expansion for any average property A is given by

$$\langle A \rangle = \langle 0|A|0\rangle + \int e^{-i\omega t} \langle\langle A; V \rangle\rangle_\omega d\omega \tag{2.23}$$

where V is given by

$$V(\omega) = \frac{1}{2\pi} \int_{-\infty}^{\infty} e^{i\omega t} V(t) dt \tag{2.24}$$

The motivation here is to evaluate matrix element of the spin-orbit operator H_{so} (given in Eq 2.2)

$$\langle {}^1\psi | H_{so} |^3\psi \rangle \tag{2.25}$$

for a reference state (singlet), for instance an MCSCF state which is a linear combination of configuration state functions(CSF)

$$|0\rangle = \sum_m C_i \Pi_i \rangle \tag{2.26}$$

without going into detail we give here the final expressions (more rigorous algebra can be found in Ref [54]).

$$\langle {}^1\psi | H_{so} |^3\psi(M_s) \rangle = \sum_{pq} h_{pq}^{M_s} \langle {}^1\psi | s_{pq}^0 |^3\psi(0) \rangle \tag{2.27}$$

With the availability of electron density based formalisms - DFT [84, 85] for the ground state and consequently time-dependent DFT[86] for excited states, response properties are also available in the DFT scheme. (See Casida for the linear response technique [87, 88, 89] and first application of LR formalism dating back to 1980[90])

Later pioneering implementations of the response technique in quantum chemistry for case of frequency-dependent nonlinear properties were developed by Scandinavian groups - the DALTON[51] and DIRAC[66] suite of programs. Salek *et al.* have used the variational principle approach based on *Ehrenfest Theorem* and *quaisenergy ansatz*[83, 91, 92]. A range of nonlinear properties like polariziability, hyper-polarizability, two-photon absorption and magnetic properties like spin-forbidden transition - as in the case of phosphorescence, magnetic circular dichorism, EPR and NMR properties now became available through response formalism [83, 93, 94, 95, 96, 97].

In this work we have used DFT based spin-orbit response theory for the computations of SOC matrix elements in chapter V and for phosphorescence in chapter VI.

2.8 DFT - Perturbation techniques

In the regular DFT method, the SOC effect can be included approximately by perturbation theory. Often a simplified operator of the type (Eq 2.3) is used

to express the SOC effect. Pederson-Khanna presented a simple approach to introduce Eq 2.3 as a perturbation.

2.8.1 Pederson-Khanna method

The potential energy matrix elements is here evaluated with single-electron wave functions, $\psi_{is} = \sum_{j\sigma} C_{j\sigma}^{is} \phi_j(r)\chi_\sigma$ (with notations used by Pederson and Khanna [29])whereas the potential energy is given by

$$U = -\frac{1}{2c^2} L \cdot S \times \nabla\phi(r) \tag{2.28}$$

an approximations which is valid for a spherically symmetric potential. The form of the potential energy matrix with SOC is thus given by

$$U_{j\sigma,k,\sigma`} = \langle \phi_j \chi_\sigma | U | \phi_k \chi_{\sigma`} \rangle \tag{2.29}$$

The second-order correction to the total energy is then

$$\Delta_2 = \sum_{\sigma,\sigma'} \sum_{i,j} M_{i,j}^{\sigma\sigma'} S_i^{\sigma\sigma'} S_j^{\sigma'\sigma} \tag{2.30}$$

whereas the matrix elements are expanded as

$$M_{i,j}^{\sigma\sigma'} = -\sum_{k,l} \frac{\langle \phi_{l\sigma} | U_i | \rangle_{k\sigma'} \langle \phi_{k\sigma'} | U_j | \phi_{l\sigma} \rangle}{\epsilon_{l\sigma} - \epsilon_{k\sigma'}} \tag{2.31}$$

and

$$S_i^{\sigma\sigma'} = \langle \chi^\sigma | S_i | \chi^{\sigma'} \rangle \tag{2.32}$$

where χ^σ and $\chi^{\sigma'}$ are the spinors, $\phi_{l\sigma}$ and $\phi_{k\sigma'}$ are occupied and unoccupied orbitals with corresponding energies $\epsilon_{l\sigma}$ and $\epsilon_{k\sigma'}$, respectively.

The above second-order shift in terms of anisotropy tensors is

$$\Delta_2 = \sum_{xy} \gamma_{xy} \langle S_x \rangle \langle S_y \rangle \tag{2.33}$$

After proper choice of co-ordinate system and diagonalizing the anisotropy tensor

Table 2.3: ZFS of selected molecules with PK and CP techniques

Molecule	Method(Functional)	D_{SOC}	D_{SSC}	D_{tot}	Expt.	Ref.
O_2	CP(BP86)	1.58	1.60	3.18	3.9	[98]
	PK(BP86)	1.58	0.79	2.37		
$[Fe(mal)_3]$	CP	-0.11(SOC+SSC)			$\pm$ 0.12	[99]
	PK	-0.13(only SOC)				
$[Mn(acac)_3]$	CP	-2.14(SOC+SSC)			-4.52	[99]
	PK	-2.36(only SOC)				

$$\begin{aligned}\Delta_2 &= \frac{1}{3}(\gamma_{xx}+\gamma_{yy}+\gamma_{zz})S(S+1) \\ &+\frac{1}{3}(\gamma_{zz}-\frac{1}{2}(\gamma_{xx}+\gamma_{yy})) \\ &(3S_z^2-S(S+1))+\frac{1}{2}(\gamma_{xx}-\gamma_{yy})(S_x^2-S_y^2)\end{aligned} \tag{2.34}$$

Eq. 2.35 is equivalent to (discarding the isotropic term)

$$H = DS_z^2 + E(S_x^2 - S_y^2) \tag{2.35}$$

The PK method is available in NRLMOL and ORCA programs.

2.8.2 The Neese technique

Reviakine *et al.* and Neese have shown independently that the PK method fails for mono-nuclear complexes .[100] Neese *et al.* has derived the second-order contribution of SOC with sum-over state equations for the ZFS tensor given by[101](with notations of Neese *et al.*)

$$
\begin{aligned}
D_{KL}^{SOC-(0)} &= -\frac{1}{S^2}\sum_{b(S_b=S)}\Delta_b^{-1}\langle 0^{SS}|\sum_i \hat{h}_i^{K;SOC_{\hat{S}_{i,0}}}|b^{SS}\rangle \qquad (2.36)\\
&\times\langle b^{SS}|\sum_i \hat{h}_i^{L;SOC_{\hat{S}_{i,0}}}|0^{SS}\rangle\\
D_{KL}^{SOC-(-1)} &= -\frac{1}{S(2S-1)}\sum_{b(S_b=S-1)}\Delta_b^{-1}\langle 0^{SS}|\sum_i \hat{h}_i^{K;SOC_{\hat{S}_{i,+1}}}|b^{S-1S-1}\rangle\\
&\times\langle b^{S-1S-1}|\sum_i \hat{h}_i^{L;SOC_{\hat{S}_{i,-1}}}|0^{SS}\rangle\\
D_{KL}^{SOC-(+1)} &= -\frac{1}{S+1)(2S+1)}\sum_{b(S_b=S+1)}\Delta_b^{-1}\langle 0^{SS}|\sum_i \hat{h}_i^{K;SOC_{\hat{S}_{i,-1}}}|b^{S+1S+1}\rangle\\
&\times\langle b^{S+1S+1}|\sum_i \hat{h}_i^{L;SOC_{\hat{S}_{i,+1}}}|0^{SS}\rangle
\end{aligned}
$$

Here $\Delta_b = E_b - E_0$ gives the excitation energy from the ground state to multiplet b. In line with Neese paper one has to emphasize here "that this is an exact analytical form of the *D-tensor* and thus modelling of any SMM does not necessarily need high spin-complex(independent of S) and it depends on the negative value of D".[102] The expression above with the *mean-field approximation* for two-electron integrals were used as discussed in section 2.3

We refer to Ref. [98] for a detailed derivation of Eq 2.37 in a conventional SCF DFT scheme. The final form after inclusion of proper prefactors for different spin excitations is given by

$$
\begin{aligned}
D_{K,L}^{0} &= \frac{1}{4S^2}\sum_{\mu\nu}\langle\mu|h_{k;so}|\nu\rangle\left(\sum_{i_\alpha,a_\alpha}U_{a_\alpha i_\alpha}^{L;0}c_{\mu i}^{\alpha}c_{\mu a}^{\alpha}\sum_{i_\alpha,a_\beta}U_{a_\beta i_\beta}^{L;0}c_{\mu i}^{\beta}c_{\mu a}^{\beta}\right) \qquad (2.37)\\
D_{K,L}^{-1} &= \frac{1}{2S(2S-1)}\sum_{\mu\nu}\langle\mu|h_{k;so}|\nu\rangle\left(\sum_{i_\alpha,a_\beta}U_{a_\beta i_\alpha}^{L;-1}c_{\mu i}^{\alpha}c_{\mu a}^{\beta}\sum_{i_\beta,a_\alpha}U_{a_\alpha i_\beta}^{L;-1}c_{\mu i}^{\beta}c_{\mu a}^{\alpha}\right)\\
D_{K,L}^{+1} &= \frac{1}{2(S+1)(2S+1)}\sum_{\mu\nu}\langle\mu|h_{k;so}|\nu\rangle\left(\sum_{i_\alpha,a_\beta}U_{a_\beta i_\alpha}^{L;+1}c_{\mu i}^{\alpha}c_{\mu a}^{\beta}\sum_{i_\beta,a_\alpha}U_{a_\alpha i_\beta}^{L;+1}c_{\mu i}^{\beta}c_{\mu a}^{\alpha}\right)
\end{aligned}
$$

In treating SSC in DFT, the McWeeny and Mizuno equation was used.[103] One should note that the PK method would be a special case of above equation Eq 2.38

$$
\begin{aligned}
D^{0}_{K,L} &= D^{-\alpha\alpha}_{K,L} + D^{-\beta\beta}_{K,L} \qquad (2.38)\\
&= \frac{1}{4S^2}\sum_{i_\alpha,a_\alpha}\langle\psi^{\alpha}_{i}|h_{K,so}|\psi^{\alpha}_{a}\rangle U^{L;0}_{a_\alpha i\alpha} + \frac{1}{4S^2}\sum_{i_\beta,a_\beta}\langle\psi^{\beta}_{i}|h_{K,so}|\psi^{\beta}_{a}\rangle U^{L;0}_{a_\beta i_\beta}\\
D^{-1}_{K,L} &= D^{\alpha\beta}_{K,L}\\
&= -\frac{1}{4S^2}\sum_{i_\alpha,a_\beta}\langle\psi^{\alpha}_{i}|h_{K,so}|\psi^{\beta}_{a}\rangle U^{L;-1}_{a_\beta i\alpha}\\
D^{+1}_{K,L} &= D^{\alpha\beta}_{K,L} \qquad (2.39)\\
&= -\frac{1}{4S^2}\sum_{i_\beta,a_\alpha}\langle\psi^{\beta}_{i}|h_{K,so}|\psi^{\alpha}_{a}\rangle U^{L;+1}_{a_\alpha i\beta}
\end{aligned}
$$

All the methods above including the PK is implemented in the ORCA quantum chemistry program from the Neese group.[104]. However, this method is not general and further development in this aspect is in progress for *D-tensor* computations[105]. For chapters 5 and 6 we have used this technique for ZFS computations.

2.9 Other approaches

Recently Yoshizawa *et al* have derived ZFS formulae to calculate the spin-orbit contribution to the ZFS with two-component self-consistent-field procedures with the second-order DKH Hamiltonian and Møller-Plesset perturbation theory.[106] A model SOC Hamiltonian were constructed by Iuchi *et al.* for computing ZFS of Ni^{2+} d-d excited states in water using molecular-dynamics simulations.[107]. It is evident from the discussed method that theoretical field for ZFS computations is broad. Regarding the association with molecular magnetism it is expected that further development in sophisticated theoretical tools will be introduced in coming years.

Chapter 3

Benchmark - Tmm and Oxyallyl

3.1 Objective

Two of the simplest diradicals - Trimethylenemethane(TMM) and oxyallyl(OXA), where the dipole-dipole like interaction is dominant compared to other orbital interactions(spin-orbit), were chosen to benchmark the methodological treatment of ZFS calculations. A multi-configurational based approach for the calculation of ZFS splitting tensors is used and results for two isoelectronic systems compared.

3.2 Biradical

3.2.1 TMM

Belonging to the D_{3h} point group symmetry, TMM is the simplest non-Kekulé conjugated structure. The ground state electronic configuration follows Hund's rule forming a triplet state ($^3B_2$) with unpaired electrons in each of two degenerate orbitals, defining it as a 'diradical'. A low-lying open-shell singlet lies above the triplet ground state separated by 1.17 eV.[108] Dowd [109, 110] first observed the planar triplet ground state geometry and later Lund *et.al* [111] reported the ESR spectrum of TMM. The molecular orbital picture clearly indicates that the diradicals of this type have multireference character of electronic configurations and hence more than one Slater-type determinant is needed to describe the eigenvalues of the triplet ground state. A detailed computational study of TMM with a multireference (up to to the level of MCSCF-[10,10]) theoretical analysis was reported by Cramer in

1966, elucidating the spectrum of different multiplets with planar and twisted structure[112]

The spin density is pre-dominantly located at the two carbon centers. The degeneracy of triplet spin densities are lifted with interactions through the spin-Hamiltonian as described in Chapter 2 The experimental ESR splitting parameter for the triplet ground state is 0.0248 cm^{-1}. Davidson *et al.* carried out the first theoretical calculations for ESR spectral splitting of TMM. A simple single Slater determinant and semi-empirical type of calculations were then employed to model the D and E parameters.[113]

3.2.2 OXA

OXA is an important intermediate in many different chemical processes and is chemically unstable. The geometrical structure virtually resembles TMM - replacing one methyl group with oxygen in TMM. Thus they are isoelectronic with oxygen replacing the total eight electrons of a methyl group(CH_2). Many experimental and theoretical investigations have predicted the triplet state as the ground state for OXA, however, recent experiment shows that singlet is the ground state multiplicity of OXA.[114] Recently, a very detailed study has been reported by Krylov*et. al* for the theoretical computation and analysis of the observed spectrum.

A single Slater determinant representation for the prediction of the ground state energy would be the precursor for any highly correlated methods in quantum chemistry. In some cases reasonably good equilibrium ground state geometries can be obtained with a single Slater determinant. If we start filling the orbitals with electrons following the Hund's rule we end up in an electronic configuration in the case of TMM as:

$$...4e_1^{'4}1a_2^{'2}1e_x^{''1}1e_y^{''1} \tag{3.1}$$

In the case of OXA:

$$...1b_1^2b_1^12a_2^1 \tag{3.2}$$

where Eq. 3.1 and Eq 3.2 are represented in D_3h and C_{2v} point group symmetry. A schematic picture of respective molecular orbitals(MOs) is shown in Refs. [115, 114, 116]. The MO picture clearly depicts that electron occupation over the MO's are essentially of *multireference character*, meaning we

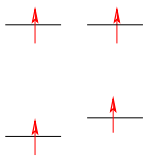

Figure 3.1: Triplet representation for TMM and OXA

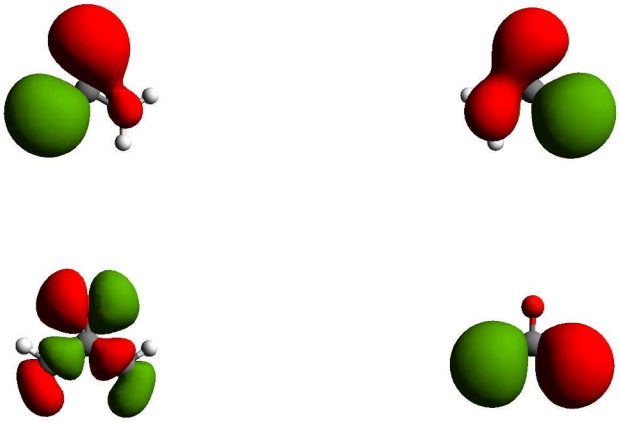

Figure 3.2: TMM and OXA triplet orbitals (SOMO's)

need more than one single determinant for minimally representing approximate ground state wavefunctions for the molecules and for corresponding energies. Accordingly we choose here the [2,2], [4,4] and [10,10] active spaces for the so-called complete active space (CAS) calculations.

The triplet ground state of TMM is $^3A_2$, whereas it is $^3b_1$ for OXA in their respective point group symmetry. Note that the OXA ground state is singlet labeled as $^1A_1$, which has been experimentally verified using photoelectron spectrum(PES) measurements[114]. The singlet-triplet gap ($^3b_1$ - $^1a_1$) is given by 0.06 eV or 480 cm^{-1}. Interestingly, if we *ignore* the zero-point energy vibrational (ZPE) corrections, then the triplet lies below the singlet of OXA. In other words if we include the ZPE corrections the singlet would be below the triplet, forming the ground state. Hence the ZPE vibrational correction alone is large enough to take the system multiplicity from singlet to triplet, thus a preference to stay away from each other would result in more stability. Such theoretical observations were also reported by Krylov*et. al.*[116] The small *singlet-triplet* energy gap comparable with ZPE corrections indicates a tendency for spontaneous conversation from the

singlet ground state to the low lying triplet. Such spontaneous process often forms a basis of an Intersystem Crossing (ISC) something that is widely studied in many optical processes (like for the carotein molecules found in mamalian eyes). Thus the singlet ground state of OXA is extremely unstable owing to its dynamic structural instability, in opposite to TMM.

In this context, the interaction studies due to SOC among close lying singlet-triplet multiplets were studied. We performed spin-orbit calculations between the singlet and triplet states for the expectation value of the type $\langle {}^1a_1|H_{so}|{}^3b_2\rangle$ at the respective geometries of singlet and triplet. We found that they are negligible and would hardly have any role in energy corrections due to SOC. (Perhaps it would be interesting study the role of SOC between these two states as a function of different reactions co-ordinates for the system. Indeed such studies were carried out for the case of TMM. [117], but our concerns were mainly focused on spin interactions at the respective triplet state in order to compare them, hence we performed SOC calculations to know its contribution at the ground state geometry). Also the typical nature of the organic system, where p-orbitals (lower orbital angular momentum shells) seldom enhances the spin-orbit interactions. Hence we narrow down the spin interactions studies of the triplet state for the other term - SSC, which is often dominant in organic species.

The obtained CAS wavefunctions, which is also a spin eigenfunction of triplet rank were subject to the electron spin-spin interaction Hamiltonian as given in chapter 2. Without this perturbation the triplet eigenstate would remain virtually degenerate and there would be no ZFS tensors classifying the triplet spectra observed from EPR measurements. The calculated D tensor for TMM is 0.02 cm^{-1} and -0.06 cm^{-1} for OXA. Owing to the D_{3h} symmetry there should be no E tensor, which often characterize the axial symmetry of the system. However, as expected we did get a small value E = -0.003 cm^{-1} for the case of OXA, signifying the symmetry breaking and assuming the lower C_{2v} point group. As we see, the above numbers for D and E are a measure of the splitting of the triplet state for the respective molecule as shown in the Paper I. An important feature is revealed if we know the sign of the tensor, i.e. the M_s=0 sub-level lies below or above of M_s=$\pm$1 with respect to the sign. We observe that there surprisingly is a spin-reversal although both have iso-electronic structure. This is well depicted in Paper I. The reason for this is attributed to the paramagnetic nature of oxygen, i.e. the negative spin-density is more predominant at the oxygen centers, where, as for the case of TMM, the electron spin is accumulated at any two of carbon centres (methyl group). The main cause of reversal of sign is due to Coulombic repulsion of the electrons. One of the essential criteria for a high-spin complex molecular magnet is D<=0, since a negative D would

give a magnetic anisotropy barrier in a model quantum double well potential with a magnitude given by $|D|S^2$. Although the splitting magnitude for this prototype species is very trivial to compare with a typical molecular magnet, a negative D might have significance in understanding and achieving better design of organic molecular magnets.

Lineberger *et. al* have reported photoelectron measurements and the vibronic strucutre of the low-lying electronic states of OXA.[118] Their study identified the vibrational spectral assignment of the $\tilde{X}^1A_1$, $\tilde{a}^3B_2$, $\tilde{b}^3B_1$ electronic states of OXA to the $\tilde{X}^2A_2$ ground state of OXA, with the support of electronic structure calculations using DFT, CASSCF and CASPT correlation procedures. Kuzmanich *et. al* observed open-shell singlet OXA through femtosecond pump-probe studies in solution and crystalline solid state of Cyclobutanedione precursor revealing a blue transient line ($\lambda_{max} = 500$) with half-life of 42 min at 298K [119]. Krylov *et. al* have carefully investigated the electronic structure and spectroscopy of OXA with comparison of the initial experimental work of Lineberger and coworkers.[116] Saito *et. al* have compared the broken symmetry and multireference coupled cluster methods for the potential energy curve for ring-opening reactions[120]

3.3 Summary

The D tensor depends on the radical spin density at the centres and the distance between them. However although we have isoelectronic structures and almost similar geometrical structures we observe a spin-reversal in OXA system compared to TMM. We also performed calculations of SOC between the singlet ground state and low lying triplet states. We found that there is negligible coupling interaction between these states at the singlet ground state geometry.

Chapter 4

Benchmark - Nitroxide Radicals

4.1 Objective

In a recent experimental discovery Okada *et al* have reported high-spin organic molecules which are stable at room temperature.[121]. In this project we have used a DFT reference to compute the ZFS of triplet degeneracy for these newly discovered nitroxide molecules.

4.2 High-Spin radical

In the previous work the molecules were small enough to be treated with multireference methods. In this work a larger sized radical was chosen for demonstration of the ZFS computational methodologies involving DFT functionals. The specific choice of the molecule(fig. 4.1) for our studies are nitroxide radicals which are TMM derivatives - discussed in the previous chapter. The striking similarity of the iso-electronic structure with the same physical and chemical properties of being a radical [121] prompted us to choose such a system for our investigation. According to the experimental group who reported the radicals, the nitroxide-substituted nitronyl nitroxide and iminonitroxide are stable at room temperature with large positive exchange interactions [121](+390 K and +550 K respectively). This study may help confirming the results of these newly discovered radicals. The fig. 4.1 depicts the geometrical structure of nitroxide- substituted nitronyl nitroxide and iminonitroxide.

The experimental ZFS tensor was obtained from an empirical fit of EPR spectra. Here we model the ZFS tensors from full *ab-initio* calculations along

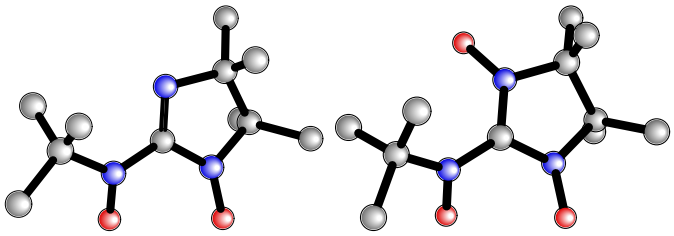

Figure 4.1: Nitroxide Biradicals

Radical	Atom	Density ρ
I	O	0.5
	N	0.3
II	O	0.30 - 0.54
	N	0.25 - 0.32

Table 4.1: Table for spin-density over atomic centers

with a theoretical verification by means of *g-tensor* calculations. The main principle of the methodologies is discussed in detail in chapter 2. Mainly, the ZFS tensors are calculated using the Kohn-Sham determinant wave function. In this case hybrid B3LYP, pure PBE functionals and local density approximations were chosen. The spin density-matrix gives the tensor components and in turn the magnitudes of D and E. The whole procedure is to evaluate the expectation value of

$$\langle {}^3\Psi_0 | H_{ss} | {}^3\Psi_0 \rangle \tag{4.1}$$

where ${}^3\Psi_0$ is the Kohn-Sham determinant.

We employ a single-determinant reference represented by a restricted open-shell configuration.and thus avoid an unrestricted open-shell type which is notorious for spin-contamination. On the other hand, geometries are often better represented with unrestricted methods, since $E_{Un} < E_{Res}$, and are thus employed in our geometry optimizations. Here the spin-contamination value for geometry optimization is around ~ 0.0010. ($\langle S^2 \rangle$)

The table 4.1 presents the distribution of the spin-density matrix over the two radicals. As we see the spin-densities are mostly distributed over the oxygen atoms. A previous study predicts that the D and E tensor for oxygen atom is 3.96 cm^{-1} and 1.44 cm^{-1} respectively, signifying a relatively high contribution for the spin coupling from oxygen centers. For both radicals we predict negative sign for the ZFS tensors, hence the M_s=0 sublevel lies above the two degenerate M_s=$\pm$1 sublevels (just like in oxyallyl case). The calculated tensors have an excellent agreement with above reported experiments. For radical I the D tensor value is close the experimental value; for the GGA

and LDA functionals, the calculated D tensor for radical II overestimate by ∼1.5 times. In this work we also calculate the *g-tensor* with our restricted linear response formalism and compared with experiments. While doing so the spin-orbit corrections, mass-velocity corrections were also accounted for i.e. the *g-tensor* components are decomposed into

$$g = g_e\hat{I} + \Delta g_{RMC} + \Delta g_{GC(1e)} + \Delta g_{GC(2e)} + \Delta g_{OZ/SO(1e)} + \Delta g_{OZ/SO(2e)} \quad (4.2)$$

where the Δ term indicates the amount of shift in the *g-tensor*. The individual terms means Δg_{RMC} mass-velocity correction term $\Delta g_{GC(xe)}$ gauge correction term $\Delta g_{OZ/SO(xe)}$ spin-orbit correction term

As the table for the *g-tensor* shift infers, these terms are sensitive to the geometries. We here emphasize that the experiments were performed in frozen diethylphthalate while the calculations were done in gas- phase. However, we obtain a consistent variation for the shift and see that inclusion of spin polarization effects give better accuracy.

4.3 Summary

This work predicts ZFS tensors for some newly discovered organic biradicals which exhibit large positive exchange interactions and which are stable at room-temperature. Although we have used only the spin-spin Hamiltonian, completely neglecting the spin-orbit, (Breit-pauli interactions), the obtained anisotropy parameters for these systems are well in agreement with experiments. The g-tensors were also computed with the restricted linear response formalism and compared with experiments.

Chapter 5

Nanographene Fragments

5.1 Objective

The elegant two-dimensional network of carbon atoms in the form of graphene is fascinating in many aspects, perhaps it is 'the material of this century' that science has given already. In many ways graphene outcompetes its silicon counterparts. In the chase of finding new properties in graphene, magnetism in graphene seems promising for novel applications. In this work we have attempted with our theoretical approach to explain the intrinsic magnetism in nanographene fragments.

5.2 Introduction

Ever since the discovery of Graphene[122] there has been huge fascination towards this simple atomic scale material. This is due to the remarkable properties associated with graphene, i.e) i) graphene sheets can conduct electricity better than conventional copper, ii) graphene has the property of a zero-gap semiconductor or zero-density of states metal at the Fermi-level, iii) it is has become a testing ground for many quantum phenomena, iv) it possesses stronger mechanical properties that outcompete steel. Though laboratory findings yet have to reach real-world practical applications, the confidence is ever growing in the industry that graphene will reach the market within a few years[123, 124]

In line with many interesting properties of graphene, magnetism is an important property to be explored. Generally, magnetism arises due to partially occupied spin polarization of d and f orbitals - in the case of carbon the magnetic signature is essentially due to the p orbital angular momentum. Since electrons are occupied in lower angular momentum orbitals(p) it

is expected that magnetism in carbon materials is weak. The findings of magnetism in graphene and in carbon in general still remains controversial.[125] Here we have attempted to explain magnetic features from the fundamental building blocks of graphene. i.e. poly-aromatic hydrocarbons (PAHs) and nanographene fragments(fig 5.2). In doing so we have used our spin-spin Hamiltonian approach discussed in Chapter 2. Such a nanographene fragment approach was also used to explain hyperfine splittings by Yazyev *et al.*[126]. The effect of the reduced dimensions on magnetism has also been predicted in a recent work in Ref.[125] Radovic *et al.* have predicted graphene edge magnetism in a series of PAH's and associated nanofragment structures.[127] Bendikov *et al.* have made a detailed analysis on PAHs starting from the case of Benzene.[128] Their work analyzes molecular orbital and electronic band structure with respect to the number of benzene rings. Motivated by the above work we have performed spin-interaction studies on such nano graphene structures starting from the PAHs. We have used a DFT based ZFS evaluation to interpret and reason the possible origin of magnetism in nanographene fragments. As far as our understanding this is the first report that discusses graphene magnetism through spin-Hamiltonian studies, in particular using the quantum chemistry perspective.

5.3 PAH's and Symmetry

First here we discuss the case of PAH's and other carbon species. Bendikov *et al.* analyze the linear PAH rings with respect to molecular orbital and band structure theory. [127]. Their predictions were based on the evidence from open-shell DFT, CASSCF, CASPT electron correlation procedures. As

Magnetic anisotropy predictions and measurements using susceptibility experiments, for benzene and other aromatic molecules, dates back to the 1930's (for example L. Pauling work on diamagnetic anisotropy of benzene[129]). Raman and Krishnan [130], Lonsdale[131] made measurements of magnetic anisotropy of benzene derivatives and aromatic molecules.

we mentioned earlier there is also a theoretical report on edge magnetism of graphene using PAH fragments. One has to be reminded that in the above work unrestricted DFT procedures were used. The main reason behind using UDFT is that unrestricted methods gives better energies than restricted. Since PAHs and many graphene fragments are highly symmetric a careful analyze is needed in dealing with symmetry. It is expected that the

unrestricted open-shell calculations break the spin symmetry. i.e. different wave-vectors for alpha and beta spin of electrons are obtained. The total electron spin-density is given by[132]

$$\rho_{tot} = \rho_{\alpha} - \rho_{\beta} \tag{5.1}$$

The side-effect for better energies in UDFT reads spin-contamination. The symmetry breaking may also concern the nuclear coordinates of the system. Hence unrestricted methods needs a careful interpretation. In a classical paper, E. Davidson points out [133] "Broken symmetry structures may appear as minima on a calculated potential surface for several reasons. One of the most common is that the calculations is *'wrong'*. That is, the form assumed for the wave function is oversimplified and leads to artefactual structure on the potential surface". Davidson *et al.* emphasized from their analysis using *Jahn-Teller distortions* (with TMM, cyclobutadiene, cyclopentadienyl cation) and *Von Neumann-Wigner Distortions* (with NO2, 1,3-dimethylnenecyclobutadiene) the artefactual nature of the broken symmetry approach for the Hartree-Fock wave-functions, also MCSCF or the limited CI approach, too suffer from small artefactual character.[133] Here we emphasize that although our geometries are from UDFT the response calculations indeed is done with restricted reference of a singlet state. Thus the question of broken spin symmetry is inherently avoided by the use of restricted procedures. Furthermore, the symmetry breaking is carefully avoided by the use of symmetry independent co-ordinates for the SOC calculations and hence use of D_{2h} point group is forced on the fragments (see appendix in paper 3 for symmetry independent co-ordinates).

Nevertheless, the mathematical machineries for the response calculations from the unrestricted references need to explored and perhaps limited for property calculations like magnetism. But, setting away from the theoretical significance of the proper description of the system, the main points to stress here is the size dependency of the magnetism on graphene fragments from restricted and unrestricted methods. We find, irrespective of the restricted or unrestricted scheme, that the single-triplet energy does decrease in the longer limit, perhaps approaching the condensed phase band structure as described in Ref [127]. The spin-density distributes well enough to avoid any short range interactions to have significant dipolar coupling.

(A beautiful atomic scale imaging of pentacene single molecules in which meticulous details of the atomic bonds and bonded orbitals at the Fermi level are revealed in high-resolution Atomic Force Microscopy(AFM), reported recently by IBM researchers[134]) Pentacene thin films are often used in organic p-type semiconductors.[135] The largest members of the acenes have been

elusive for some time. Recently, Bettinger and coworkers have synthesized pentacene, hexacene and heptacene crystals and investigated their spectral and thermal stability.[136]

The singlet-triplet energy gap of linear PAHs approaches a fixed value ($0.25\ eV$) for the size $n > 7$ at B3LYP/6-31G(d) calculations.[127] The two polyacetylene $-C = CH - C = CH - C = CH-$ chains are connected by a single C-C bond in the sp^2 hybridized planar PAH structure. This is explained by the absence of the *Peierls distortion* of each polyacetylene chain.

In our work linear PAH's, until $n = 10$, were optimized and these structures were further subject to spin-Hamiltonian studies, in particular the spin-dipole interactions and spin-orbit interactions (discussed in Chapter 2. The parametrized representation of such interactions are tabulated and some of them are compared with experiment. The most important analogy we draw from these numbers is the strong decrease in the *D-tensor* strength as depicted in fig. 5.1.

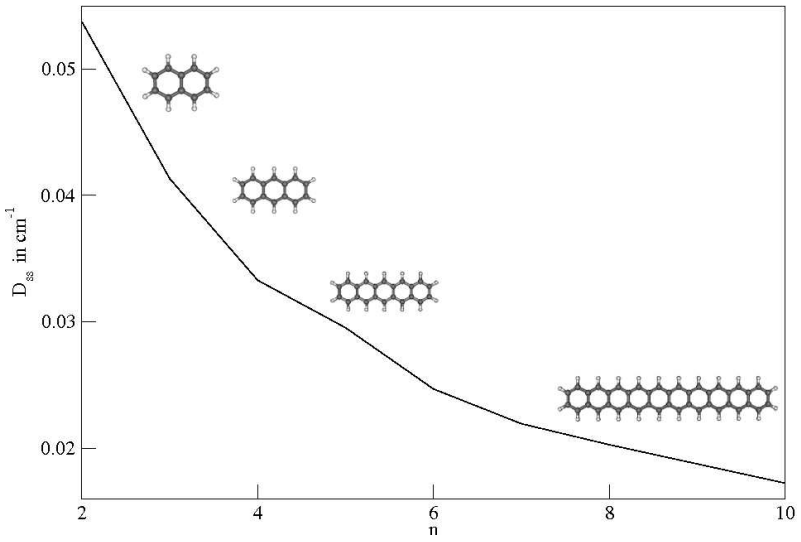

Figure 5.1: Spin-spin tensor D_{ss} dependence of linear polyacene size

The linear response spin-orbit interaction from the ground state A_g to the lowest triplet state ($^3B_{1g}$, $^3B_{2g}$ and $^3B_{3g}$ were presented for the linear PAHs, in order to realize the magnitude of the spin-orbit matrix element between the molecular singlet-triplet orbitals. From these results we could draw two-important conclusions, firstly, that irrespective of the size of the

[1]a broken symmetry in one-dimensional lattice and hence oscillation over the equilibrium

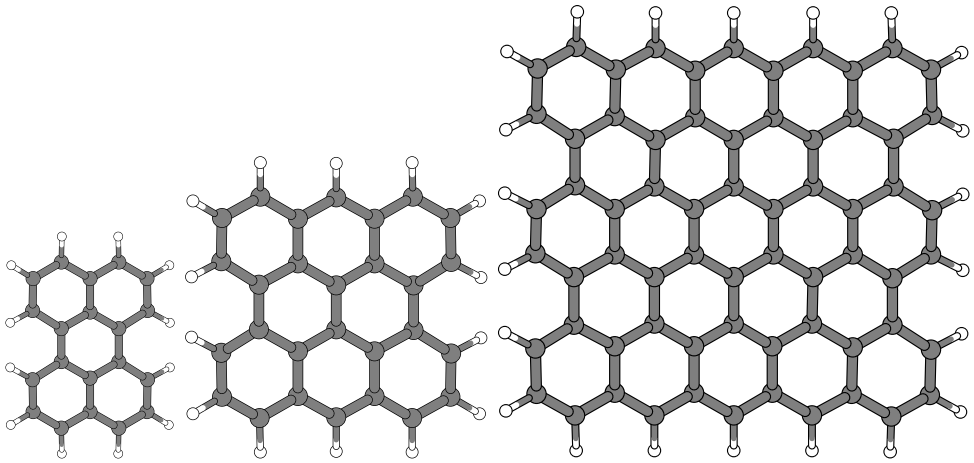

Figure 5.2: 2×3, 3×3 and 5×5 nanographene fragments

π conjugation the SSC dominates for this system and the D_{ss} tensor alone can effectively reproduce the EPR splitting. Secondly, there exists a strong pattern of correlation between the number of the rings and dipole-dipole interactions. Wholgenannt and Rybicki predicted a relativistic contribution for π conjugated polymer chains as 10 μeV,[137] and our calculations of $10 - 20$ μeV were in good agreement with their results.

5.4 Nanofragments

Small sized nanofragments were studied by Nakano *et al.* [138, 139] for correlating the second hyperpolarizability(γ) and the diradical nature of the model fragments. The similar systems were predicted to have anti-ferromagnetic spin ordering.[140, 141]. Here we have constructed similar model fragments (PAH[3,3],PAH[5,5] fig. 5.2) and applied our spin calculations, similarly as for the linear PAHs. The ground states were predicted to have singlet multiplicity and the singlet and low-lying triplet geometries and energies are in good agreement with previous literature values [142, 143, 144]. Again there seems to be size dependence of the ribbons that is evident from our calculations. As size increases the spin densities are dominant more around the zigzag edges of the fragments.

Similar to the square graphene fragments as described above we have have constructed *triangulenes* in line with theoretical and experimental works of Morita and co-workers.[145, 146] (triangulene structures are shown in fig. 5.3). The significant aspect one has to note here is in fig. 5.3; all the species possess non-bonding (π) MOs with *non-disjoint* degenerate charac-

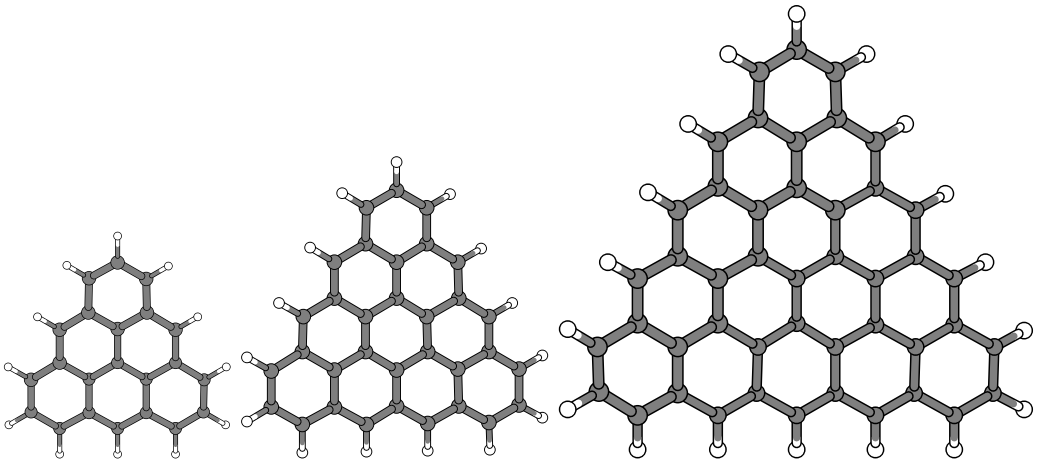

Figure 5.3: Triangular ribbons

ter. And their ground state spin magnetic moment varies with size.[147] Our calculated parameters D = 0.01554 cm^{-1}, E = 0 cm^{-1} for the triplet ground state of the triangulene very close to those Morita and co-workers reports for triangulene derivatives with three *tert*-butyl groups i.e) |D| = 0.0073 cm^{-1}, E $\simeq$ 0 cm^{-1}. Though large scale triangulenes have not been isolated experimentally, their high-spin ground state multiplicity could possibly be used in magnetic applications.

We have introduced a single defect in the PAH[5,5] model nanographene fragments - a very simple approximation for the vacancy effect in the square graphene species. The introduced defect can be compared with the non-distorted structure strongly perturbed as is revealed by the change of the E parameter and by the increase in the SSC, approximately by an order of magnitude. The spin-density cartoon in fig. 5.4 shows accumulation of spin on the edges in the vicinity of the defect.

5.5 Analogue fragments

The Boron nitride graphene models are constructed by replacing each C-C bond with a B-N bond. Similar construction is used for the former carbon nanographene flakes to generate Boron nitride ribbons(BNNR). All these BNNR models have a singlet closed-shell ground state with relatively high S_0-T_1 energy gap. Thus their triplet state properties can be related to ultraviolet photochemistry. Similar to linear polyacenes we performed our calculations on linear BNNRs. single-layered n-rings model. BNNRs are found to have a significant S_0-T_1 energy gap, whereas the former have zero band-gap for

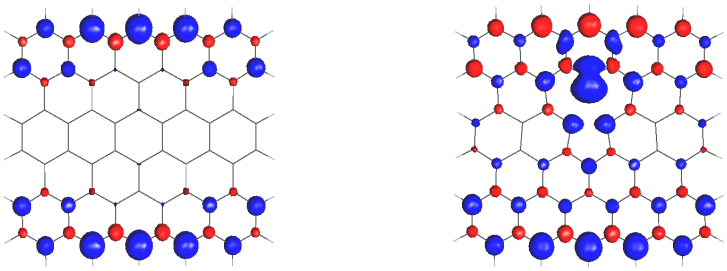

Figure 5.4: Spin density of graphene nanoribbons with a defect - contour drawn with isovalue 0.05

large n in agreement with previous calculations. We predict BNNRs to be magnetic non-metallic materials.

Since Then The graphenes possess remarkable properties, like the Dirac points or cones - where the graphene conduction and valence bands meet. And hence the Dirac-Hamiltonian is often used to describe its characteristic features. It was thought that the two-dimensional honey-comb lattice with equivalent carbon lattice was responsible for such a Dirac cone band-structure. However, with a recent first principle evidence Görling[148] and co-workers points out that the existence of Dirac-cones behavior does not necessarily depend on the hexagonal structures and such behavior do exist in other two-dimensional carbon structures like graphynes, 6,6,12-graphyne which has no hexagonal symmetry. Thus their study reveals many other equivalent candidates possessing similar interesting properties as graphene.

5.6 Summary

In summary, we have constructed model graphene ribbons from the basic unit of benzene and applied them for our spin-Hamiltonian approach. The triplet SSC seems to have a significant size dependency with respect to the number of rings. The problem of broken symmetry in unrestricted schemes is discussed with implication to our spin studies. We propose that considerable intrinsic magnetism in nanographene fragments can be associated only with defects and impurities.

Chapter 6

Alq3 - modelling the magnetic switch

6.1 Objective

Tris-hydroxy Aluminium 8-oxalate is a well known material among optical chemists and physicists. The high efficiency fluorescence of Alq3 has been utilized in everyday applications such as in LED. This material has been proved experimentally to act as magnetic switches and play the role of buffers between magnetic sandwiches. [149] In paper 4 we tried to model the triplet states of the Alq_3 molecule and SOC effectis to improve our understanding of the experimental observations.

6.2 Triplet-Singlet transitions

The pioneering discovery by Van Alyck facilitated the production of the efficient LED material Alq_3 that is widely available in commercial use now.[150] In a significant recent breakthrough, the Alq_3 molecule has been demonstrated to have spintronic applications at low temperature. Magnetoresistance (MR) - a process in which change in resistance of the material is triggered by a change in alignment of spins in ferromagnetic layers, has been observed in NiFe/LiF/Alq3/FeCo layers[149]. The magnetoresistance measurement is significant in the sense that spin-injection is possible with introduction of LiF thin-films. The main reasons for the passage of polarized spin is due to tuning of molecular orbitals of Alq_3 in the presence of LiF. A self-explanatory magnetoresistance vs magnetic field has been reported in Ref [149]. Although the Alq_3 molecule has been famous for its electroluminescence applications for some time, the phosphorescence of Alq_3 was elusive for

long until irecent reports by Burrows *et al.* and Cölle *et al.* independently reported observations of phosphorescence. [151, 152, 153]. Later Tanaka *et al.* have observed strong phosphorescence with energy transfer from iridium complexes.[154] In an interesting report Yu has reported relatively strong SOC (2.75×10^{-2} for negatively charged Alq_3) compared to similar organic species of Benzene, Rubrene, Phenylenevinylen and Sexithiophene.[155] In this context it is important to study SOC effects, the source of phosphorescence, in Alq_3.

Label	Singlet	Triplet
	Bond length(Å)	
Al(1)-O(18)	1.855	1.851
Al-O(35)	1.881	1.867
Al-O(52)	1.884	1.963
Al-N(2)	2.084	2.105
Al-N(19)	2.126	2.123
Al-N(36)	2.064	1.994
	Angle	
N(2)-Al-N(36)	171.5	170.1
N(19)-Al-O(18)	172.7	172.35
O(52)-Al-O(35)	166.6	168.06

Table 6.1: Geometries parameter of ground state and triplet state of Alq_3 at ub3lyp/6-31G(d) (label shown in the fig. 6.1)

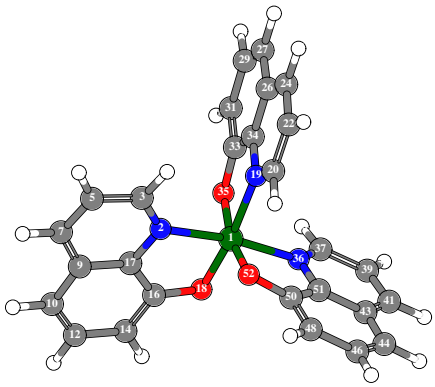

Figure 6.1: Alq3 molecule

The Al_3 molecule has three quionlate ligands as shown in the fig. 6.1 which prominently contribute to the π contribution. The geometries of the

ground state Al_3 molecule is presented in Table 6.1 and our results are consistent with previous DFT studies.[151, 156, 157, 158] Here we have calculated ten singlet and ten triplet excited states with linear response theory. The singlet energies and triplet energies are in good agreement with the previous theoretical and experimental work.[151, 152, 159]

Functional	Method	D_{ss}	E_{ss}	D_{so+ss}	E_{so+ss}	$\langle S^2 \rangle$ - $S(S+1)$
B3LYP	CP	0.02252	0.00290	0.01734	0.00513	0.02535
B3LYP	QRO	0.04539	0.00124	0.08489	0.00450	0.02535
BP86	CP	-0.02337	0.01697	-0.01873	-0.00485	0.01088
BP86	QRO	0.03829	-0.00245	0.09034	0.00900	0.01088
Expt.[152]	$\|D\| = 0.0630$	$\|E\| = 0.0114$				

Table 6.2: ZFS parameters (in cm^{-1}) for first triplet state of Alq_3

For the first triplet state we have computed ZFS, earlier measured experimentally by Cölle *et al.* Our ZFS calculations are based on the method outlined in Chapter 2. The experimental ZFS parameter values of 0.0630 cm^{-1} and 0.0114 cm^{-1} are in close agreement with our results (refer Table 6.2). Since the experimental observations of phosphorescence of Alq_3 were obtained in benzene solvent, we have used here PCM model for benzene to mimic the benzene environment. In order to study the influence of the LiF layer on Alq_3 we have introduced an LiF molecule in the vicinity of Alq_3. Indeed these are very simple approximations, nonetheless we are here mainly motivated to study the possible tuning of MO's of Alq_3 and the SOC effect. Such assumptions are also reported in theoretical modelling the electronic structure of Alq_3 in pristine.[160] The calculated radiative lifetime is presented in the Table 6.3. The radiative lifetime in gas phase for the T_4-S_0 and T_5-S_0 are 11.5 *ms* and 2.6 *ms* respectively, which is in the range of measured lifetime of 7 *ms*. Hence, the low-lying triplet states from our calculation do not contribute to the spin-forbidden transitions. With the account of vibrational corrections(here we refer to nuclear motions with respective to the multiplet geometry) a mixing of low-lying triplet and upper triplet states could be revealed. With the inclusion of benzene environment we obtain a similar trend in radiative lifetime as in the gas phase. We also obtain considerable radiative lifetime in the higher states as well.(Ref. 6.3) In conclusion, the SOC effect in Alq_3 for the spin-forbidden transitions is very weak owing to the weak coupling contribution of the aluminum.

6.2.1 Spin-injection

In the presence of a polar molecule (LiF) the electric-dipole moment has a pronounced enhancement (4.4 debye to 8.7 debye) which is mainly due to the additive property of the dipole moment (dipole moment of LiF is ~ 5 debye) and this indicates a significant electrical field anisotropic effect introduced by the LiF molecule, which essentially leadis to altering of the energy levels of the molecular orbitals of Alq_3. This effect is indeed a desirable feature in tuning the valence MO's for the spin-injection to pass throughi; the dipole moment introduced by LiF is here the cause of vacuum level shifts of the MO's of Al_3.[149] Although a single LiF may not mimic a realistic picture of thin-films of LiF, the polar effect is indeed captured at the molecular level. There seems to be a small amount of gain amount of the Mulliken charges in the aluminum atom in the presence of LiF. ($\sim 1.15\ |e|$ for 'Alq_3 + LiF' and '$\sim 0.98\ |e|$ for Alq_3). The shift in energies of the HOMO was found to be of the order of ~ 0.05 eV with respect to the presence of LiF. These findings are significant as Schulz*et al.* have reported spin-injection(*mainly hole-injection through the HOMO's of* Alq_3) operating at less than 100 mV.[149]

6.3 Summary

To summarize, we have for the first time theoretically explored the phosphorescence of the Alq_3 molecule. We predict the lifetime be 11 ms, 2.6 ms for triplet states of energies 2.79 eV and 2.95 eV, respectively, in gas phase. With benzene environment lifetimes of 1.7 ms and 2.3 ms were obtained. This is in reasonable agreement with experimental phosphorescence decay of 7 ms from the first low-lying triplet state of energy 2.05 eV from Ref. [151] The DFT ZFS calculations are also in very good agreement with the ODMR measurements. Finally we have theoretically predicted the shift in the MO's of Alq_3 molecule in the presence of polar LiF, which is in line with the experimental magnetoresistance report for spin-injection signatures.[149]

Triplet State	Transition rate (in s^{-1})			Lifetime (τ_k) (S)		
	in gas phase	in Benzene	near LiF	in gas phase	in Benzene	near LiF
1	0.277×10^{-3}	0.404×10^{-3}	0.545	36.073	24.745	18.346
2	0.276×10^{-3}	0.523×10^{-3}	0.438	36.255	19.110	22.838
3	0.278×10^{-3}	0.318×10^{-3}	0.110	35.929	31.429	9.104
4	86.580	600.920	5.923	0.116×10^{-3}	1.664×10^{-3}	0.169
5	386.330	438.410	3.795	2.588×10^{-3}	2.281×10^{-3}	0.263
6	5.025	2.369	21.929	0.199	0.42221	0.456×10^{-3}
7	5.431	37.107	14781	0.184	0.269×10^{-3}	0.677×10^{-6}
8	5.283	8.288	23.077	0.190	0.121	0.433×10^{-3}
9	8.290	62.012	0.235	0.121	0.161×10^{-3}	4.2505
10	17.883	0.261	773	0.559×10^{-3}	3.833	1.294×10^{-3}

Table 6.3: Radiative lifetime of triplet states at the S_0 geometry

Chapter 7

Conclusion and Future perspective

It is almost a century since the first theory for electron spin was put forward. The mathematical machinery of this relativistic theory is by now well established. Though earlier development of main stream ab-initio calculations was focused on post-Hartree-fock schemes without relativistic effects, the importance of relativistic effects in quantum chemistry has successively been stressed along with the use of gaussian type basis sets.[20] The prediction of relativistic properties of interest, in particular spectral splittings, has been made possible for a range of molecular species of different size and character.

In recent years the theoretical development has been mainly driven by the motive to achieve novel material design. Studies on spin-interaction (and hence relativistic effects) as the driving mechanism for molecular-level magnetism is gaining attention. The introduction of density functional theory has to some extent overshadowed the remarkable achievement in post-Hartree-fock methods, and has by now developed to an attractive approach in the design of functional materials. DFT for spin properties has greatly spurred applications on magnetism. In this work we have outlined applications of the relativistic Hamiltonian both in multireference and DFT based implementations, in particular for the prediction of anisotropy parameters for molecular magnetism. The advantages and shortcomings are highlighted for the various implementations. We have benchmarked these approaches for organic species where in general the anisotropy parameter predictions largely have been successful. Our primary examples in this respect were the isoelectronic diradicals Oxyallyl and TMM. We explained the triplet degeneracy splitting with the use of the SSC Hamiltonian, where our results were found to be in good agreement with recent experiments. We here explored a spin-reversal

behavior in triplet state splittings, which may be significant in designing organic magnetic switches. Our study also confirmed that SSC dominates in organic species. Newly discovered nitroxide radicals which exhibit large positive exchange interactions and which are stable at room temperature were subject to our spin- Hamiltonian studies.

With these two benchmarks as basis we have used our methodologies to predict the magnetic behavior of nanographene fragments through their anisotropy parameters. The dependence on size of the (very small) non-intrinsic magnetic field in the nanographene fragments were predicted in our calculations. The importance of proper interpretation of spin unrestricted and restricted DFT and the consequences of broken symmetry in such two-dimensional systems is emphasized. We predicted that nanographene magnetism can only be realized by impurities and defects in these systems. We extended the procedures to BN nanographenes and could predict that such BN fragments should be magnetic non-metallic materials.

We reported phosphorescence calculations for the first time for the Alq_3 molecule. The triplet states are energetically in good agreement with the observations and our ZFS tensor numbers were found to be in line with OLED measurements. The tuning of molecular orbitals of the Alq_3 molecule with the presence of LiF polar molecules was also very well accounted for in our calculations. This feature has recently been observed for spin-injection properties in metal/organic sandwich layers. Overall, the methodologies used here were successful in prediction of anisotropy parameters. There is certainly need for new techniques to handle higher spin multiplicities with judicious computational usage for calculating two-electron SOC integrals with proper excited reference states. The Neese technique appears to be the most successful method available for anisotropy parameter predictions for now. We have also performed preliminary calculations on anisotropy parameters for the case of Fe-metallopthalocyanine. A detailed analysis on this highly symmetric system is under progress. Also the spin-flip TDDFT approach by Krylov et al. seems promising in dealing with proper description of excited reference states.[161, 162] Possible SOC implementation in spin-flip DFT remains an attractive choice for prediction of singlet-triplet SOC coupling in DFT.

With all these developments, quantum chemical spin-interaction studies hold the promise as an exciting research field of interest both in academic research and for applications in the search of functional materials of technological relevance.

Bibliography

[1] V. Vedral. *Decoding Reality: the universe as quantum information*. Oxford Univ Pr, 2010.

[2] R. Bradshaw and C. Schroeder. Fifty years of ibm innovation with information storage on magnetic tape. *IBM Journal of Research and Development*, 47(4):373–383, 2003.

[3] P. Grünberg, R. Schreiber, Y. Pang, MB Brodsky, and H. Sowers. Layered magnetic structures: Evidence for antiferromagnetic coupling of fe layers across cr interlayers. *Physical Review Letters*, 57(19):2442–2445, 1986.

[4] MN Baibich, JM Broto, A. Fert, F. Nguyen Van Dau, F. Petroff, P. Etienne, G. Creuzet, A. Friederich, and J. Chazelas. Giant magnetoresistance of(001) fe/(001) cr magnetic superlattices. *Physical Review Letters*, 61(21):2472–2475, 1988.

[5] R. Sessoli, D. Gatteschi, A. Caneschi, and MA Novak. Magnetic bistability in a metal-ion cluster. *Nature*, 365(6442):141–143, 1993.

[6] D. Gatteschi and R. Sessoli. Molecular nanomagnets: the first 10 years. *Journal of Magnetism and Magnetic Materials*, 272:1030–1036, 2004.

[7] O. Kahn. Molecular magnetism. *VCH Publishers, Inc.(USA), 1993,*, page 393, 1993.

[8] D. Gatteschi, R. Sessoli, and J. Villain. *Molecular nanomagnets*. Oxford University Press, USA, 2006.

[9] W. Wernsdorfer. Classical and quantum magnetization reversal studied in nanometer-sized particles and clusters. *Handbook of Advanced Magnetic Materials*, pages 77–127, 2006.

[10] A.V. Postnikov, J. Kortus, and M.R. Pederson. Density functional studies of molecular magnets. *Physica Status Solidi (b)*, 243(11):2533–2572, 2006.

[11] A. Caneschi, D. Gatteschi, R. Sessoli, A.L. Barra, L.C. Brunel, and M. Guillot. Alternating current susceptibility, high field magnetization, and millimeter band EPR evidence for a ground S= 10 state in [$Mn_{12}O_{12}$ (CH_3COO) 16

(H_2O) 4]. $2CH_3COOH$. $4H_2O$. *Journal of the American Chemical Society*, 113(15):5873–5874, 1991.

[12] C.J. Milios, A. Vinslava, W. Wernsdorfer, A. Prescimone, P.A. Wood, S. Parsons, S.P. Perlepes, G. Christou, and E.K. Brechin. Spin switching via targeted structural distortion. *Journal of the American Chemical Society*, 129(20):6547–6561, 2007.

[13] J. Krzystek, G.J. Yeagle, J.H. Park, R.D. Britt, M.W. Meisel, L.C. Brunel, and J. Telser. High-frequency and-field epr spectroscopy of tris (2, 4-pentanedionato) manganese (iii): Investigation of solid-state versus solution jahn-teller effects. *Inorganic chemistry*, 42(15):4610–4618, 2003.

[14] M. Dressel, B. Gorshunov, K. Rajagopal, S. Vongtragool, and AA Mukhin. Quantum tunneling and relaxation in mn 12-acetate studied by magnetic spectroscopy. *Physical Review B*, 67(6):060405, 2003.

[15] R. Boča. Zero-field splitting in metal complexes. *Coordination Chemistry Reviews*, 248(9-10):757–815, 2004.

[16] C. van Wullen. Magnetic anisotropy from density functional calculations. Comparison of different approaches: MnO acetate as a test case. *The Journal of Chemical Physics*, 130:194109, 2009.

[17] H. Lefebvre-Brion and R.W. Field. Perturbations in the spectra of diatomic molecules. 1986.

[18] A. Abragam and B. Bleaney. *Electron paramagnetic resonance of transition ions*. Clarendon Press Oxford, 1970.

[19] P. Pyykko. Relativistic effects in structural chemistry. *Chemical Reviews*, 88(3):563–594, 1988.

[20] P. Pyykko and J.P. Desclaux. Relativity and the periodic system of elements. *Accounts of Chemical Research*, 12(8):276–281, 1979.

[21] R. Ahuja, A. Blomqvist, P. Larsson, P. Pyykkö, and P. Zaleski-Ejgierd. Relativity and the lead-acid battery. *Physical Review Letters*, 106(1):18301, 2011.

[22] K. Balasubramanian. *Relativistic effects in chemistry*, volume 1. Wiley, 1997.

[23] P. Pyykko. Relativistic effects: They re more important than you think. *Annual Review of Physical Chemistry*, 63(1), 2012.

[24] P. Pyykko. The physics behind chemistry and the periodic table. *Chemical Reviews-Columbus*, 112(1):371, 2012.

[25] D.G. Fedorov, S. Koseki, M.W. Schmidt, and M.S. Gordon. Spin-orbit coupling in molecules: chemistry beyond the adiabatic approximation. *International Reviews in Physical Chemistry*, 22(3):551–592, 2003.

[26] C.M. Marian. Spin-orbit coupling in molecules. *Reviews in computational chemistry*, pages 99–204, 2001.

[27] J. Autschbach. Perspective: Relativistic effects. *The Journal of chemical physics*, 136(15):150902, 2012.

[28] J. Kortus, M.R. Pederson, T. Baruah, N. Bernstein, and CS Hellberg. Density functional studies of single molecule magnets. *Polyhedron*, 22(14-17):1871–1876, 2003.

[29] MR Pederson and SN Khanna. Magnetic anisotropy barrier for spin tunneling in $Mn_{12}O_{12}$ molecules. *Name: Physical Review, B: Condensed Matter*, 60:13, 1999.

[30] L. Bogani and W.L. Wernsdorfer. Molecular spintronics using single-molecule magnets. *Nature materials*, 7(3):179–186, 2008.

[31] P. Gambardella, S. Rusponi, M. Veronese, SS Dhesi, C. Grazioli, A. Dallmeyer, I. Cabria, R. Zeller, PH Dederichs, K. Kern, C. Carbone, and H. Bruen. Giant magnetic anisotropy of single cobalt atoms and nanoparticles. *Science*, 300(5622):1130–1133, 2003.

[32] T. Balashov, T. Schuh, AF Takacs, A. Ernst, S. Ostanin, J. Henk, I. Mertig, P. Bruno, T. Miyamachi, S. Suga, et al. Magnetic anisotropy and magnetization dynamics of individual atoms and clusters of Fe and Co on Pt (111). *Physical review letters*, 102(25):257203, 2009.

[33] T.O. Strandberg, C.M. Canali, and A.H. MacDonald. Transition-metal dimers and physical limits on magnetic anisotropy. *Nature materials*, 6(9):648–651, 2007.

[34] D. Fritsch, K. Koepernik, M. Richter, and H. Eschrig. Transition metal dimers as potential molecular magnets: A challenge to computational chemistry. *Journal of Computational Chemistry*, 29(13):2210–2219, 2008.

[35] P. Błoński and J. Hafner. Magnetic anisotropy of transition-metal dimers: Density functional calculations. *Physical Review B*, 79(22):224418, 2009.

[36] P. Błonski, S. Dennler, and J. Hafner. Strong spin–orbit effects in small pt clusters: Geometric structure, magnetic isomers and anisotropy. *The Journal of Chemical Physics*, 134:034107, 2011.

[37] L. Fernández-Seivane and J. Ferrer. Magnetic anisotropies of late transition metal atomic clusters. *Physical review letters*, 99(18):183401, 2007.

[38] R. Xiao, D. Fritsch, M.D. Kuzmin, K. Koepernik, H. Eschrig, M. Richter, K. Vietze, and G. Seifert. Co dimers on hexagonal carbon rings proposed as subnanometer magnetic storage bits. *Physical review letters*, 103(18):187201, 2009.

[39] R. Xiao, D. Fritsch, M.D. Kuzmin, K. Koepernik, M. Richter, K. Vietze, and G. Seifert. Prediction of huge magnetic anisotropies of transition-metal dimer-benzene complexes from density functional theory calculations. *Physical Review B*, 82(20):205125, 2010.

[40] M. Sargolzaei and F. Gudarzi. Magnetic properties of single 3d transition metals adsorbed on graphene and benzene: A density functional theory study. *Journal of Applied Physics*, 110:064303, 2011.

[41] VA Rigo, RH Miwa, A.J.R. da Silva, and A. Fazzio. Mn dimers on graphene nanoribbons: An ab initio study. *Journal of Applied Physics*, 109:053715, 2011.

[42] S.D. Jiang, B.W. Wang, H.L. Sun, Z.M. Wang, and S. Gao. An organometallic single-ion magnet. *Journal of the American Chemical Society*, 2011.

[43] R. Sessoli and A.K. Powell. Strategies towards single molecule magnets based on lanthanide ions. *Coordination Chemistry Reviews*, 253(19-20):2328–2341, 2009.

[44] D.P. Mills, F. Moro, J. McMaster, J. van Slageren, W. Lewis, A.J. Blake, and S.T. Liddle. A delocalized arene-bridged diuranium single-molecule magnet. *Nature Chemistry*, 3(6):454–460, 2011.

[45] A.S. Zyazin, J.W.G. van den Berg, E.A. Osorio, H.S.J. van der Zant, N.P. Konstantinidis, M. Leijnse, M.R. Wegewijs, F. May, W. Hofstetter, C. Danieli, et al. Electric field controlled magnetic anisotropy in a single molecule. *Nano letters*, 2010.

[46] E. Ruiz, J. Cirera, J. Cano, S. Alvarez, C. Loose, and J. Kortus. Can large magnetic anisotropy and high spin really coexist? *Chemical Communications*, (1):52–54, 2008.

[47] SJ Blundell and FL Pratt. Organic and molecular magnets. *Journal of Physics: Condensed Matter*, 16:R771, 2004.

[48] P. Day and A.E. Underhill. *Metal-organic and organic molecular magnets*. Number 252. Springer Us/Rsc, 1999.

[49] A. Rajca. Organic diradicals and polyradicals: From spin coupling to magnetism? *Chemical reviews*, 94(4):871–893, 1994.

[50] H.M. McConnell. A theorem on zero-field splittings. *Proceedings of the National Academy of Sciences of the United States of America*, 45(2):172, 1959.

[51] DALTON - 2.X, an ab initio electronic structure program, 2011. See the DALTON manual at http://daltonprogram.org.

[52] B.A. Hess, C.M. Marian, U. Wahlgren, and O. Gropen. A mean-field spin-orbit method applicable to correlated wavefunctions. *Chemical Physics Letters*, 251(5-6):365–371, 1996.

[53] C.M. Marian and U. Wahlgren. A new mean-field and ECP-based spin-orbit method. Applications to Pt and PtH. *Chemical Physics Letters*, 251(5-6):357–364, 1996.

[54] O. Vahtras, H. Ågren, P. Jørgensen, H.J.A. Jensen, T. Helgaker, and J. Olsen. Spin–orbit coupling constants in a multiconfiguration linear response approach. *The Journal of Chemical Physics*, 96(3):2118, 1992.

[55] T. Reuters.

[56] S. Koseki, M.S. Gordon, M.W. Schmidt, and N. Matsunaga. Main group effective nuclear charges for spin-orbit calculations. *The Journal of Physical Chemistry*, 99(34):12764–12772, 1995.

[57] S. Koseki. Spin-orbit coupling effects in di-hydrides of third-row transition elements. In *Computational methods in science and engineering: theory and computation: old problems and new challenges, lectures presented at the International Conference on Computational Methods in Science and Engineering 2007 (ICCMSE 2007), Corfu, Greece, 25-30 September 2007*, volume 1, page 257. Amer Inst of Physics, 2007.

[58] S. Koseki, D.G. Fedorov, M.W. Schmidt, and M.S. Gordon. Spin-orbit splittings in the third-row transition elements: Comparison of effective nuclear charge and full breit-pauli calculations. *The Journal of Physical Chemistry A*, 105(35):8262–8268, 2001.

[59] S. Koseki, M.W. Schmidt, and M.S. Gordon. MCSCF/6-31G (d, p) calculations of one-electron spin-orbit coupling constants in diatomic molecules. *The Journal of physical chemistry*, 96(26):10768–10772, 1992.

[60] S. Koseki, M.W. Schmidt, and M.S. Gordon. Effective nuclear charges for the first-through third-row transition metal elements in spin-orbit calculations. *The Journal of Physical Chemistry A*, 102(50):10430–10435, 1998.

[61] C.M. Marian. Spin-orbit coupling and intersystem crossing in molecules. *Computional Molecular Science*, pages 187–203, 2012.

[62] P.A.M. Dirac. The quantum theory of the electron. *Proc. R. Soc. London. Series A, Containing Papers of a Mathematical and Physical Character*, 117(778):610–624, 1928.

[63] PJC Aerts and WC Nieuwpoort. On the optimization of gaussian basis sets for hartree-fock-dirac calculations. *Chemical physics letters*, 125(1):83–90, 1986.

[64] O. Visser, PJC Aerts, D. Hegarty, and WC Nieuwpoort. The use of gaussian nuclear charge distributions for the calculation of relativistic electronic wavefunctions using basis set expansions. *Chemical physics letters*, 134(1):34–38, 1987.

[65] L. Visscher, O. Visser, P.J.C. Aerts, H. Merenga, and WC Nieuwpoort. Relativistic quantum chemistry: the molfdir program package. *Computer physics communications*, 81(1-2):120–144, 1994.

[66] DIRAC, a relativistic ab initio electronic structure program, Release DIRAC11 (2011), (see http://dirac.chem.vu.nl).

[67] J. Gao, W. Liu, B. Song, and C. Liu. Time-dependent four-component relativistic density functional theory for excitation energies. *The Journal of chemical physics*, 121:6658, 2004.

[68] Z. Li, W. Liu, et al. Spin-adapted open-shell random phase approximation and time-dependent density functional theory. i. theory. *The Journal of chemical physics*, 133(6):064106, 2010.

[69] Z. Li, W. Liu, Y. Zhang, and B. Suo. Spin-adapted open-shell time-dependent density functional theory. ii. theory and pilot application. *The Journal of chemical physics*, 134:134101, 2011.

[70] Z. Li and W. Liu. Spin-adapted open-shell time-dependent density functional theory. iii. an even better and simpler formulation. *Journal of Chemical Physics*, 135(19):194106, 2011.

[71] Z. Li and W. Liu. Theoretical and numerical assessments of spin-flip time-dependent density functional theory. *Journal of Chemical Physics*, 136(2):24107, 2012.

[72] T. Yanai, T. Nakajima, Y. Ishikawa, and K. Hirao. A highly efficient algorithm for electron repulsion integrals over relativistic four-component gaussian-type spinors. *The Journal of chemical physics*, 116:10122, 2002.

[73] T. Yanai, T. Nakajima, Y. Ishikawa, and K. Hirao. A new computational scheme for the dirac–hartree–fock method employing an efficient integral algorithm. *The Journal of Chemical Physics*, 114:6526, 2001.

[74] T. Yanai, H. Nakano, T. Nakajima, T. Tsuneda, S. Hirata, Y. Kawashima, Y. Nakao, M. Kamiya, H. Sekino, and K. Hirao. Utchema program for ab initio quantum chemistry. *Computational ScienceICCS 2003*, pages 712–712, 2003.

[75] L. Belpassi, L. Storchi, H.M. Quiney, and F. Tarantelli. Recent advances and perspectives in four-component dirac–kohn–sham calculations. *Phys. Chem. Chem. Phys.*, 13(27):12368–12394, 2011.

[76] W. Kutzelnigg. Perturbation theory of relativistic corrections. ii: Analysis and classification of known and other possible methods. *Zeitschrift für Physik. D, atoms, molecules and clusters*, 15(1):27–50, 1990.

[77] G. Te Velde, F.M. Bickelhaupt, E.J. Baerends, C. Fonseca Guerra, S.J.A. van Gisbergen, J.G. Snijders, and T. Ziegler. Chemistry with adf. *Journal of Computational Chemistry*, 22(9):931–967, 2001.

[78] F. Martyn, I.J. Bush, H.J.J. Van Dam, P. Sherwood, J.M.H. Thomas, J.H. Van Lenthe, R.W.A. Havenith, and J. Kendrick. The gamess-uk electronic structure package: algorithms, developments and applications. *Molecular physics*, 103(6-8):719–747, 2005.

[79] Michael W. Schmidt, Kim K. Baldridge, Jerry A. Boatz, Steven T. Elbert, Mark S. Gordon, Jan H. Jensen, Shiro Koseki, Nikita Matsunaga, Kiet A. Nguyen, Shujun Su, Theresa L. Windus, Michel Dupuis, and John A. Montgomery. General atomic and molecular electronic structure system. *J. Comput. Chem.*, 14(11):1347–1363, November 1993.

[80] M. S. Gordon and M. W. Schmidt. *Advances in electronic structure theory: GAMESS a decade later*, pages 1167–1189. Elsevier, Amsterdam, 2005.

[81] T. Nakajima and K. Hirao. The douglas-kroll-hess approach. *Chemical reviews*, 112:385–402, 2012.

[82] M. Reiher. Relativistic douglas–kroll–hess theory. *Wiley Interdisciplinary Reviews: Computational Molecular Science*, 2011.

[83] J. Olsen and P. Jørgensen. Linear and nonlinear response functions for an exact state and for an mcscf state. *The Journal of chemical physics*, 82:3235, 1985.

[84] W. Kohn and Sham. *Self-consistent equations including exchange and correlation effects*. APS, 1965.

[85] P. Hohenberg and W. Kohn. Inhomogeneous electron gas. *Physical Review*, 136(3B):B864, 1964.

[86] E. Runge and E.K.U. Gross. Density-functional theory for time-dependent systems. *Physical Review Letters*, 52(12):997–1000, 1984.

[87] M.E. Casida, C. Jamorski, K.C. Casida, and D.R. Salahub. Molecular excitation energies to high-lying bound states from time-dependent density-functional response theory: Characterization and correction of the time-dependent local density approximation ionization threshold. *The Journal of chemical physics*, 108:4439, 1998.

[88] ME Casida and DP Chong. Recent advances in density functional methods, part i. *Recent Advances in Computational Chemistry*, 1:155, 1995.

[89] JM Seminario. *Recent developments and applications of modern density functional theory*, volume 4. Elsevier Science, 1996.

[90] A. Zangwill and P. Soven. Density-functional approach to local-field effects in finite systems: Photoabsorption in the rare gases. *Physical Review A*, 21(5):1561, 1980.

[91] J.E. Rice and N.C. Handy. The calculation of frequency-dependent polarizabilities as pseudo-energy derivatives. *The Journal of chemical physics*, 94:4959, 1991.

[92] C. Hättig, J. Jørgensen, and O. Christiansen. *Int. J. Quantum Chem*, 68:1, 1998.

[93] O. Vahtras, B. Minaev, and H. Ågren. Ab initio calculations of electronic g-factors by means of multiconfiguration response theory. *Chemical Physics Letters*, 281(1-3):186–192, 1997.

[94] Z. Rinkevicius, L. Telyatnyk, P. Sałek, O. Vahtras, and H. Ågren. Restricted density-functional linear response theory calculations of electronic g-tensors. *The Journal of Chemical Physics*, 119:10489, 2003.

[95] I. Tunell, Z. Rinkevicius, O. Vahtras, P. Sałek, T. Helgaker, and H. Ågren. Density functional theory of nonlinear triplet response properties with applications to phosphorescence. *The Journal of chemical physics*, 119:11024, 2003.

[96] O. Loboda, B. Minaev, O. Vahtras, B. Schimmelpfennig, H. Ågren, K. Ruud, and D. Jonsson. Ab initio calculations of zero-field splitting parameters in linear polyacenes. *Chemical Physics*, 286(1):127–137, 2003.

[97] O. Vahtras, O. Loboda, B. Minaev, H. Ågren, and K. Ruud. Ab initio calculations of zero-field splitting parameters. *Chemical Physics*, 279(2-3):133–142, 2002.

[98] F. Neese. Calculation of the zero-field splitting tensor on the basis of hybrid density functional and Hartree-Fock theory. *The Journal of Chemical Physics*, 127:164112, 2007.

[99] J. Cirera, E. Ruiz, S. Alvarez, F. Neese, and J. Kortus. How to build molecules with large magnetic anisotropy. *Chemistry-A European Journal*, 15(16):4078–4087, 2009.

[100] R. Reviakine, A.V. Arbuznikov, J.C. Tremblay, C. Remenyi, O.L. Malkina, V.G. Malkin, and M. Kaupp. Calculation of zero-field splitting parameters: Comparison of a two-component noncolinear spin-density-functional method and a one-component perturbational approach. *The Journal of chemical physics*, 125:054110, 2006.

[101] F. Neese and E.I. Solomon. Articles-Calculation of Zero-Field Splittings, g-Values, and the Relativistic Nephelauxetic Effect in Transition Metal Complexes. Application to High-Spin Ferric Complexes. *Inorganic Chemistry*, 37(26):6568–6582, 1998.

[102] F. Neese and D.A. Pantazis. What is not required to make a single molecule magnet. *Faraday Discuss.*, 2010.

[103] R. McWeeny and Y. Mizuno. The density matrix in many-electron quantum mechanics. ii. separation of space and spin variables; spin coupling problems. *Proc.R. Soc. London. Series A. Mathematical and Physical Sciences*, 259(1299):554–577, 1961.

[104] F. Neese. Orca. *An ab initio, density functional and semiempirical program package, University of Bonn: Bonn*, 2007.

[105] Personal communications.

[106] T. Yoshizawa and T. Nakajima. Second-order generalized unrestricted møller–plesset perturbation theory for the spin–orbit part of zero-field splitting tensors. *Chemical Physics Letters*, 2011.

[107] S. Iuchi and S. Sakaki. Spin-orbit coupling in a model hamiltonian for dd excited states of ni2+ ion aqueous solution. *Chemical Physics Letters*, 485(1-3):114–118, 2010.

[108] P.G. Wenthold, J. Hu, R.R. Squires, and WC Lineberger. Photoelectron spectroscopy of the trimethylene-methane negative ion. the singlet-triplet splitting of trimethylenemethane. *Journal of the American Chemical Society*, 118(2):475–476, 1996.

[109] P. Dowd. Trimethylenemethane. *Journal of the American Chemical Society*, 88(11):2587–2589, 1966.

[110] P. Dowd. Trimethylenemethane. *Accounts of Chemical Research*, 5(7):242–248, 1972.

[111] K. Kenji, M. Shiotani, and A. Lund. An ESR study of trimethylenemethane radical cation. *Chemical Physics Letters*, 265(1-2):217–223, 1997.

[112] C.J. Cramer and B.A. Smith. Trimethylenemethane. Comparison of Multiconfiguration Self-Consistent Field and Density Functional Methods for a Non-Kekule Hydrocarbon. *Journal of Physical Chemistry*, 100(23):9664–9670, 1996.

[113] D. Feller, W.T. Borden, and E.R. Davidson. Calculation of zero field splitting parameters for trimethylenemethane. *The Journal of Chemical Physics*, 74:2256, 1981.

[114] T. Ichino, S.M. Villano, A.J. Gianola, D.J. Goebbert, L. Velarde, A. Sanov, S.J. Blanksby, X. Zhou, D.A. Hrovat, W.T. Borden, et al. The Lowest Singlet and Triplet States of the Oxyallyl Diradical (Angew. Chem. Int. Ed. 45/2009). *Angewandte Chemie International Edition*, 48(45), 2009.

[115] L.V. Slipchenko and A.I. Krylov. Electronic structure of the trimethylenemethane diradical in its ground and electronically excited states: Bonding, equilibrium geometries, and vibrational frequencies. *The Journal of Chemical Physics*, 118:6874, 2003.

[116] V. Mozhayskiy, D.J. Goebbert, L. Velarde, A. Sanov, and A.I. Krylov. Electronic Structure and Spectroscopy of Oxyallyl: A Theoretical Study. *The Journal of Physical Chemistry A*, page 170, 2010.

[117] T.R. Furlani and H.F. King. Theory of spin-orbit coupling. application to singlet–triplet interaction in the trimethylene biradical. *The Journal of chemical physics*, 82:5577, 1985.

[118] T. Ichino, S.M. Villano, A.J. Gianola, D.J. Goebbert, L. Velarde, A. Sanov, S.J. Blanksby, X. Zhou, D.A. Hrovat, W.T. Borden, et al. Photoelectron spectroscopic study of the oxyallyl diradical. *The Journal of Physical Chemistry A*, 2011.

[119] G. Kuzmanich, F. Spanig, C.K. Tsai, J.M. Um, R.M. Hoekstra, KN Houk, D.M. Guldi, and M.A. Garcia-Garibay. Oxyallyl exposed: an open-shell singlet with picosecond lifetimes in solution but persistent in crystals of a cyclobutanedione precursor. *Journal of the American Chemical Society*, 2011.

[120] T. Saito, N. Yasuda, Y. Kataoka, Y. Nakanishi, Y. Kitagawa, T. Kawakami, S. Yamanaka, M. Okumura, and K. Yamaguchi. Potential energy curve

for ring-opening reactions: Comparison between broken-symmetry and multireference coupled cluster methods. *The Journal of Physical Chemistry A*, 2011.

[121] Shuichi Suzuki, Takanori Furui, Masato Kuratsu, Masatoshi Kozaki, Daisuke Shiomi, Kazunobu Sato, Takeji Takui, and Keiji Okada. Nitroxide-substituted nitronyl nitroxide and iminonitroxide. *Journal of the American Chemical Society*, 135(45):15908–15910, 2010.

[122] A.K. Geim and K.S. Novoselov. The rise of graphene. *Nature materials*, 6(3):183–191, 2007.

[123] http://www.guardian.co.uk/science/2011/oct/07/huge-investment-graphene-nobel-prizewinner.

[124] http://www.guardian.co.uk/business/2012/mar/18/britain-needs-innovation-economy.

[125] O.V. Yazyev. Emergence of magnetism in graphene materials and nanostructures. *Reports on Progress in Physics*, 73:056501, 2010.

[126] O.V. Yazyev. Hyperfine interactions in graphene and related carbon nanostructures. *Nano letters*, 8(4):1011–1015, 2008.

[127] M. Bendikov, H.M. Duong, K. Starkey, KN Houk, E.A. Carter, and F. Wudl. Oligoacenes: Theoretical prediction of open-shell singlet diradical ground states. *Journal of American Chemical Society*, 126(24):7416–7417, 2004.

[128] L.R. Radovic and B. Bockrath. On the chemical nature of graphene edges: Origin of stability and potential for magnetism in carbon materials. *Journal of American Chemical Society*, 127(16):5917–5927, 2005.

[129] L. Pauling. The diamagnetic anisotropy of aromatic molecules. *The Journal of Chemical Physics*, 4:673, 1936.

[130] CV Raman and K.S. Krishnan. Magnetic double-refraction in liquids. part i. benzene and its derivatives. *Proc. R. Soc. London. Series A*, 113(765):511–519, 1927.

[131] K. Lonsdale. Magnetic anisotropy and electronic structure of aromatic molecules. *Proc. R. Soc. London. Series A-Mathematical and Physical Sciences*, 159(896):149–161, 1937.

[132] A. Szabo and N.S. Ostlund. *Modern quantum chemistry: introduction to advanced electronic structure theory*. Dover Pubns, 1996.

[133] E.R. Davidson and W.T. Borden. Symmetry breaking in polyatomic molecules: real and artifactual. *The Journal of Physical Chemistry*, 87(24):4783–4790, 1983.

[134] L. Gross, F. Mohn, N. Moll, P. Liljeroth, and G. Meyer. The chemical structure of a molecule resolved by atomic force microscopy. *Science*, 325(5944):1110–1114, 2009.

[135] J.E. Anthony. The larger acenes: versatile organic semiconductors. *Angewandte Chemie International Edition*, 47(3):452–483, 2008.

[136] R. Mondal, C. Tonshoff, D. Khon, D.C. Neckers, and H.F. Bettinger. Synthesis, stability, and photochemistry of pentacene, hexacene, and heptacene: a matrix isolation study. *Journal of the American Chemical Society*, 131(40):14281–14289, 2009.

[137] J. Rybicki and M. Wohlgenannt. Spin-orbit coupling in singly charged π-conjugated polymers. *Physical Review B*, 79(15):153202, 2009.

[138] M. Nakano, H. Nagai, H. Fukui, K. Yoneda, R. Kishi, H. Takahashi, A. Shimizu, T. Kubo, K. Kamada, and K. Ohta. Theoretical study of third-order nonlinear optical properties in square nanographenes with open-shell singlet ground states. *Chemical Physics Letters*, 467(1-3):120–125, 2008.

[139] H. Nagai, M. Nakano, K. Yoneda, H. Fukui, T. Minami, S. Bonness, R. Kishi, H. Takahashi, T. Kubo, and K. Kamada. Theoretical study on third-order nonlinear optical properties in hexagonal graphene nanoflakes: Edge shape effect. *Chemical Physics Letters*, 477(4-6):355–359, 2009.

[140] Oded Hod, Veronica Barone, and Gustavo E. Scuseria. Half-metallic graphene nanodots: A comprehensive first-principles theoretical study. *Phys. Rev. B*, 77:035411, 2008.

[141] De en Jiang, Xing-Qiu Chen, Weidong Luo, and William A. Shelton. From trans-polyacetylene to zigzag-edged graphene. *Chemical Physics Letters*, 483:120, 2009.

[142] M. Huzak, MS Deleuze, and B. Hajgató. Half-metallicity and spin-contamination of the electronic ground state of graphene nanoribbons and related systems: An impossible compromise? *The Journal of Chemical Physics*, 135:104704, 2011.

[143] H. Nagai, M. Nakano, K. Yoneda, R. Kishi, H. Takahashi, A. Shimizu, T. Kubo, K. Kamada, K. Ohta, and E. Botek. Signature of multiradical character in second hyperpolarizabilities of rectangular graphene nanoflakes. *Chemical Physics Letters*, 489(4-6):212–218, 2010.

[144] S. Rayne and K. Forest. A comparison of density functional theory (dft) methods for estimating the singlet–triplet (s0-t1) excitation energies of benzene and polyacenes. *Computational and Theoretical Chemistry*, 976(1):105–112, 2011.

[145] J. Inoue, K. Fukui, T. Kubo, S. Nakazawa, K. Sato, D. Shiomi, Y. Morita, K. Yamamoto, T. Takui, and K. Nakasuji. The first detection of a clar's hydrocarbon, 2, 6, 10-tri-tert-butyltriangulene: A ground-state triplet of non-kekulé polynuclear benzenoid hydrocarbon. *Journal of the American Chemical Society*, 123(50):12702–12703, 2001.

[146] Y. Morita, S. Suzuki, K. Sato, and T. Takui. Synthetic organic spin chemistry for structurally well-defined open-shell graphene fragments. *Nature Chemistry*, 3(3):197–204, 2011.

[147] M. Ezawa. Metallic graphene nanodisks: Electronic and magnetic properties. *Physical Review B*, 76(24):245415, 2007.

[148] D. Malko, C. Neiss, F. Viñes, and A. Görling. Competition for graphene: Graphynes with direction-dependent dirac cones. *Physical Review Letters*, 108(8):086804, 2012.

[149] L. Schulz, L. Nuccio, M. Willis, P. Desai, P. Shakya, T. Kreouzis, VK Malik, C. Bernhard, FL Pratt, NA Morley, et al. Engineering spin propagation across a hybrid organic/inorganic interface using a polar layer. *Nature materials*, 2010.

[150] CW Tang and SA VanSlyke. Organic electroluminescent diodes. *Applied Physics Letters*, 51(12):913–915, 1987.

[151] H.D. Burrows, M. Fernandes, J.S. de Melo, A.P. Monkman, and S. Navaratnam. Characterization of the triplet state of tris (8-hydroxyquinoline) aluminium (iii) in benzene solution. *Journal of the American Chemical Society*, 125(50):15310–15311, 2003.

[152] M. Colle, C. Garditz, and M. Braun. The triplet state in tris-(8-hydroxyquinoline) aluminum. *Journal of applied physics*, 96(11):6133–6141, 2004.

[153] M. Colle and C. Garditz. Phosphorescence of aluminum tris (quinoline-8-olate). *Applied physics letters*, 84:3160, 2004.

[154] I. Tanaka, Y. Tabata, and S. Tokito. Observation of phosphorescence from tris (8-hydroxyquinoline) aluminum thin films using triplet energy transfer from iridium complexes. *Physical Review B*, 71(20):205207, 2005.

[155] ZG Yu. Spin-orbit coupling, spin relaxation, and spin diffusion in organic solids. *Physical Review Letters*, 106(10):106602, 2011.

[156] M. Brinkmann, G. Gadret, M. Muccini, C. Taliani, N. Masciocchi, and A. Sironi. Correlation between molecular packing and optical properties in different crystalline polymorphs and amorphous thin films of mer-tris

(8-hydroxyquinoline) aluminum (iii). *Journal of the American Chemical Society*, 122(21):5147–5157, 2000.

[157] A. Curioni, M. Boero, and W. Andreoni. Alq3: ab initio calculations of its structural and electronic properties in neutral and charged states. *Chemical Physics Letters*, 294(4-5):263–271, 1998.

[158] A. Irfan, R. Cui, and J. Zhang. Fluorinated derivatives of mer-alq3: energy decomposition analysis, optical properties, and charge transfer study. *Theoretical Chemistry Accounts: Theory, Computation, and Modeling (Theoretica Chimica Acta)*, 122(5):275–281, 2009.

[159] M. Amati and F. Lelj. Are UV–Vis and luminescence spectra of Alq_3 [aluminum tris (8-hydroxy quinolinate)] δ-phase compatible with the presence of the fac-Alq_3 isomer? A TD-DFT investigation. *Chemical physics letters*, 358(1):144–150, 2002.

[160] N. Johansson, T. Osada, S. Stafstrom, WR Salaneck, V. Parente, DA Dos Santos, X. Crispin, and JL Bredas. Electronic structure of tris (8-hydroxyquinoline) aluminum thin films in the pristine and reduced states. *The Journal of chemical physics*, 111:2157, 1999.

[161] L.V. Slipchenko and A.I. Krylov. Singlet-triplet gaps in diradicals by the spin-flip approach: A benchmark study. *The Journal of chemical physics*, 117:4694, 2002.

[162] Y. Shao, M. Head-Gordon, and A.I. Krylov. The spin–flip approach within time-dependent density functional theory: Theory and applications to diradicals. *The Journal of chemical physics*, 118:4807, 2003.

ACKNOWLEDGMENT

I have enormously benefited from self-learning. In that process many science books, open-source resources and digital tools have assisted me. While working for this thesis i have extensively used *Google scholar*, *web of knowledge*, *KTH online-library* and other open-source codes, *popular science books*, etc, i thank everyone of them for all possible available solutions for the questions i had and constantly refining my thoughts. I feel privileged to live in such a well-connected digital world and we certainly "stand on the shoulders of giants".

It was an extra challenge, concerning to this nature of this project in particularly it was also involved a new geography profile for Prof. Hans Ågren and Theoretical chemistry dept. to work with. I hope this exercise would turn up fruit full for me in the future. I specially thank Prof. Hans for that.

I acknowledge the funding support from VR Swedish Research Links in the initial years and from Prof. Hans Ågren during past one year.

I thank all the supercomputing infrastructure (PDC-KTH Stockholm, NSC Linköping, HPC Umeå, Garder Iceland) and it's excellent support group.

Prof. Boris Minaev seriousness irrespective of dimensions of discussions taught me to give extra attention towards any issues. His long professional carrier and consistent enthusiasm towards academic research, despite of personal constraints, certainly a remarkable example of passion about science. His wife Prof. Valentina occasional presence in Stockholm gave a very light moments with lots of Russian jokes in the coffee-time discussions and i personally thank Prof. Boris and his wife and Gleb for all the gifts they brought me from Ukraine.

Special thanks to Prof. Olav Vahtras and Prof. Hans Ågren for going through the summary and suggesting comments.

I thank anonymous reviewers for critical comments which definitely helped in improving our work and gave a different insight into to the project.

I would like to take this opportunity to thank Pawel, Yiu Luo, Faris, Fahmi(also for arranging nice Football play) for the course. I appreciate the helpful suggestions from Prof. Margareta, Prof. Sasha, Prof. Lakaasan while taking their quantum chemistry course in Stockholm University.

I thank Xing Chen, Weiju Hua and his wife, Giangian Tian for inviting me to a nice "Chinese supper". I thank Kai Fu for giving company to the Swimming pool in the freezing winter of Sweden.

Stockholm gave me few ever memorable friends, special thanks are due

to Ainars, Michael for helping me out during critical times.

I thank my group members in KTH, Fuming, Xing Chen, Katia for being a good colleague. I thank other members - Salam, Vsevolod, TT, Andrei, Peter, Phoneix, Keyan, Xia-Fei, Staffan(for theochem internal support), Bin Gao, Ning, Fang Qiu, Zhang, Qiong, Qiang, Yuejie Ai, Yuping, Hui cao, etc from theoretical chemistry and from other dept. for occasional chat to maintain sanity while working.

It was unforgettable moments with Prof. K. J. Rao of SSCU, IISc. Special thanks to him for all the lively passionated discussion about science and issues related to it.

I thank Prof. Chandrabhas arranging a way for funding while i was in India and his group members for showing interest to work with me. I thank Prof. Yashonath(SSCU, IISc) for a nice introduction to molecular dynamics simulation and i also thank Prof. Ramasesha(SSCU, IISc) for asking me to take this assignment initially.

There are bunch of others who made me to feel less stressful while i was in IISc, particularly i wish to express my thanks to Balaji, Ganesh, etc.

I thank all the secretarial support which was done very "professionally" from the years of Lotta to Marlene and Pia as Well.

Finally, certainly not the least, I am eternally grateful to my parents, grandmother, grandfather, brother and sister for their support through best possible means and forgiving me to spent much of the time away from them to carry out this work and readily accepting my decisions whatever i made.